Computer Modeling in Engineering & Sciences

Tech Science Press

DOI: 10.32604/cmes.2022.023694

check for updates

ARTICLE

A Detailed Mathematical Analysis of the Vaccination Model for COVID-19

Abeer S. Alnahdi[1,*], Mdi B. Jeelani[1], Hanan A. Wahash[2] and Mansour A. Abdulwasaa[3,4]

[1]Department of Mathematics and Statistics, Imam Mohammad Ibn Saud Islamic University (IMSIU), Riyadh, Saudi Arabia

[2]Department of Mathematics, Dr. Babasaheb Ambedkar Marathwada University, Aurangabad, India

[3]Department of Statistics, Taiz University, Taiz, Yemen

[4]Department of Statistics, Dr. Babasaheb Ambedkar Marathwada University, Aurangabad, India

*Corresponding Author: Abeer S. Alnahdi. Email: asalnahdi@imamu.edu.sa

Received: 09 May 2022 Accepted: 30 June 2022

ABSTRACT

This study aims to structure and evaluate a new COVID-19 model which predicts vaccination effect in the Kingdom of Saudi Arabia (KSA) under Atangana-Baleanu-Caputo (ABC) fractional derivatives. On the statistical aspect, we analyze the collected statistical data of fully vaccinated people from June 01, 2021, to February 15, 2022. Then we apply the Eviews program to find the best model for predicting the vaccination against this pandemic, based on daily series data from February 16, 2022, to April 15, 2022. The results of data analysis show that the appropriate model is autoregressive integrated moving average ARIMA (1, 1, 2), and hence, a forecast about the evolution of the COVID-19 vaccination in 60 days is presented. The theoretical aspect provides equilibrium points, reproduction number R_0, and biologically feasible region of the proposed model. Also, we obtain the existence and uniqueness results by using the Picard-Lindel method and the iterative scheme with the Laplace transform. On the numerical aspect, we apply the generalized scheme of the Adams-Bashforth technique in order to simulate the fractional model. Moreover, numerical simulations are performed dependent on real data of COVID-19 in KSA to show the plots of the effects of the fractional-order operator with the anticipation that the suggested model approximation will be better than that of the established traditional model. Finally, the concerned numerical simulations are compared with the exact real available date given in the statistical aspect.

KEYWORDS

COVID-19; Eviews program; forecasting; ABC fractional derivative; Picard-Lindel method; Adams-Bashforth technique

1 Introduction

Coronaviruses have three branches known as alpha, beta, and gamma. Recently, various strains of SARS-CoV-2 have emerged, including the most destructive and most dangerous delta variant, SARS-CoV-2 [1]. Human coronaviruses have been first distinguished during the 1960s. The first case reported of COVID-19 in Wuhan City in China's Hubei Province on December 31, 2019, has been found to be contaminated with a new COVID-19 that has never been seen. As reported [2], this disease is believed to be transmitted from animal creatures to people, like SARS-CoV and MERS-CoV. Now the

disease is sent from one individual to another. On March 23, 2022, according to the global statistics of this epidemic, the number of infected cases was estimated at 480,165,010, while the number of people recovered reached 414,597,310. By this date, there were 6,144,249 deaths related to the disease worldwide [3]. In this regard, an investigation of the patients who died found that most of them were elderly or patients who had been diagnosed with chronic diseases such as heart disease, diabetes, lung and kidney disease, etc.

Despite the different non-pharmaceutical control systems against COVID-19, a portion of the vaccines that have acquired crisis use approval (EUA) by the United States Centers for Disease Control and Prevention (CDC) are the Pfizer-BioNTech with 95% efficacy, the Moderna immunization with 94.5% viability, and the Janssen vaccine with 67% adequacy, and many others, see [4]. The vaccines have been successful against SARS-CoV-2 infections, including asymptomatic infections and symptomatic cases, severe COVID-19 disease, and deaths.

KSA began vaccinating people against the Coronavirus on December 17, 2020. On November 03, 2021, the use of the Pfizer vaccine was approved for the age groups 5–11 years. In the early stages of the vaccine, citizens and residents over 65 were targeted, which ended on February 18, 2021, whereas the second phase was launched on February 18, 2021, it targeted citizens and residents over 50 years old. The third phase targeted all citizens and residents wishing to receive the vaccine.

On the other hand, time series models are employed in the estimate process of variable behavior and other phenomena, as well as their future trends in diseases, epidemiology, climate sciences, economics, management, and other sciences. Lately, mathematical and statistical modeling have been used to forecast the behavior and patterns of some epidemics and diseases. The prediction method for these models includes four fundamental procedures, such as determining the model, estimation of unknown parameters, diagnostic process, and prediction process. The models (MA, AR, ARCH, ARMA, GARCH, ARIMA) are among the most commonly used time series models for forecasting [5–8].

In this context, the processes of making a mathematical model of a problem, interpreting the solution, validating the model, then making the model ready for utilization are not processes that can be conquered directly. Particularly these days, large numbers of the problems are complicated, nonlinear, have memory impact, or possess a stochastic construction; therefore, modeling methods and solutions specific to these problems must be developed.

Fractional calculus has shown gigantic improvement in applications to various real-world problems in different fields such as continuum mechanics, electromagnetic theory, and biological mathematics. Fractional calculus has become a substantial mathematical tool for the investigation of nonlinear derivative problems, see [9–13]. In modeling biological systems, fractional derivatives play a significant role in considering the nonlocality and memory impact properties that perfectly fit the test data of memory phenomena in various disciplines, such as mechanics, epidemiology, and psychology. The memory effect clarifies that the future condition of the fractional operator of a certain function relies upon its recorded behavior and present status. By using fractional derivatives, especially Caputo fractional derivatives, several real-world systems have been studied successfully in biomathematics and engineering [14–17]. The fractional derivative's definition has different methodologies with various kernels, so the researchers are keen on picking the best one. Specialists are drawn in by the nonsingular kernels as the classical singular kernels experienced difficulties in modeling some physical phenomena. Caputo et al. [18] overcome this trouble by expanding the Caputo fractional derivative to a nonsingular kernel. There are some interesting properties of the Caputo-Fabrizio operator that have been discussed by Losada et al. in [19]. ABC fractional derivative was given by Atangana et al. in [20], they considered

the generalized Mittag-Leffler function as a nonsingular and nonlocal kernel. Some of the generalized characteristics of the ABC operator are introduced in [21,22]. This new operator commanded the attention of investigators because of its brilliant memory description [23,24]. Recent mathematical models on COVID-19 under the ABC operator show different approaches to manifest the transmission of the disease, see [25–32]. In this regard, other papers dealt extensively with modeling and analysis of the transmission of the COVID-19 pandemic in order to limit the spread of this epidemic, see [33–38]. Diagne et al. [39] formulated a mathematical model of the COVID-19 transmission mechanism with Vaccination and Treatment. A mathematical model of COVID-19 with the effect of vaccines was constructed by Gokbulut et al. [40]. They made the analysis of the model, then the idea of vaccination was used with a change in the vaccination rate among the population. Yavuz et al. [41] developed a mathematical model to reveal the effects of vaccine treatment on COVID-19 based on a system of ordinary differential equations.

The literature shows that very few works available on COVID-19 models are in the form of ABC fractional derivatives, even though they describe the dynamic behavior accurately compared to the classical derivatives. To our knowledge, there is no available literature on the COVID-19 fractional model with an expectation of the vaccination effect on KSA. Therefore, this is the main motivation behind our work. Also, the comparison of the real data with different fractional order simulations is one of our unique aims in this work. In addition, we extend and generalize the model studied by Yavuz et al. [41], based on a system of fractional differential equations involving ABC fractional derivatives.

This work is organized as follows. Section 2 provides a statistical analysis of COVID-19 vaccination in KSA. Some background material and auxiliary results of ABC fractional calculus are given in Section 3. The fractional mathematical model and its fundamental properties are described in Section 4. In Section 5, we prove the theoretical results of the given model. Sections 6 and 7 give numerical results and simulation results by estimating the parameters. In the last section, we provide brief conclusions of the study.

2 Statistical Analysis

In this section, we discuss some empirical results. First, we analyze and present the descriptive data of the vaccinated persons in KSA. Then we predict the number of people who will be fully vaccinated during the next period.

2.1 Descriptive Data Analysis

The latest statistics about the vaccination of people against the spread of the Coronavirus epidemic are collected from the official data published by the Saudi Ministry of Health as the fully vaccinated people reached 144,057 during the period January 06, 2021, to June 27, 2021, with an average of 8,401 per day. Then, data is collected on the number of fully vaccinated people daily during the period June 28, 2021, to February 15, 2022. Table 1 indicates that the number of vaccinated people in July 2021 reached 6,493,739, with an average of 209,476 people per day. Then it increased in August 2021 to reach 6,833,828 with an average of 220,446 people per day. Hence, we observe that the number of vaccinated people decreased continuously until the number of vaccinated people during the fifteen days of February 2022 reached 264,633. In general, the number of fully vaccinated people during the studied period reached 23,964,566, which represents 67.81% of the total population in KSA, which is 35,340,680 people. For more details, see Figs. 1 and 2.

Table 1: The number of people fully vaccinated from June 01, 2021 to February 15, 2022 in KSA [42]

Months	Vaccinated people	Mean of vaccinated people
06 Jan to 27 Jun-21	1,445,087	8,401
From 28 Jun-21	142,494	47,498
Jul-21	6,493,739	209,476
Aug-21	6,833,828	220,446
Sep-21	3,807,265	126,909
Oct-21	2,789,720	89,991
Nov-21	955,376	30,819
Dec-21	713,370	23,012
Jan-22	519,054	16,744
Until 15 Feb-22	264,633	17,642
Total	23,964,566	102,852

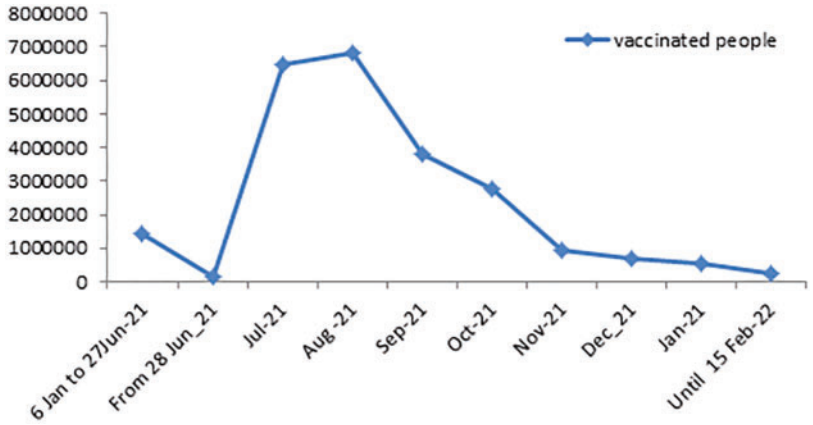

Figure 1: Number of people fully vaccinated in the KSA during the period June 01, 2021 to February 15, 2022

Table 2 summarizes the number of daily doses taken by people against coronavirus disease in KSA during the period June 28, 2021, to February 15, 2022. We find that the doses increased continuously from January 2021 to April 2021, then decreased in May 2021 and June 2021. After that, it increased dramatically in July 2021 and August 2021 to reach 19,252,318 doses with 33% of the total doses given during the study period. Then it decreased during the period from September 2021 to December 2021. The total doses given amounted to 57,964,264 during the studied period, with an average of 248,773 doses per day.

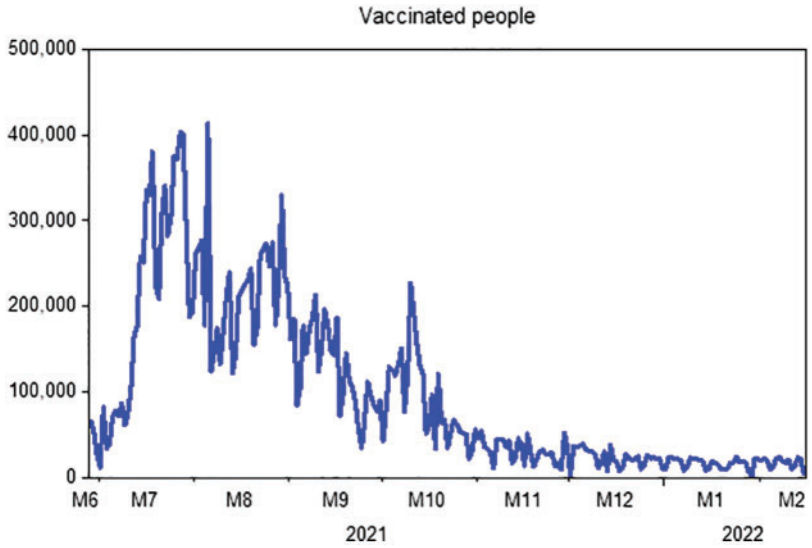

Figure 2: Daily numbers of people completed vaccinations in KSA from June 28, 2021 to February 15, 2022

Table 2: New doses for people from January 06, 2021 to February 15, 2022 in KSA [42]

Months	New doses	Mean of new doses
Jan-21	57865	1867
Feb-21	114810	4100
March-21	3475774	112122
Apr-21	4911419	163714
May-21	4864301	156913
Jun-21	3672578	122419
Jul-21	8986886	289899
Aug-21	10265432	331143
Sep-21	4976527	165884
Oct-21	3611147	116489
Nov-21	1590443	53015
Dec-21	3406053	109873
Jan-22	5697591	183793
Until 15 Feb-22	2333438	155563
Total	57964264	248773

2.2 Prediction Strategies

In this portion, we are collecting data on the fully vaccinated people in KSA for the period June 01, 2021 to February 15, 2022. Moreover, the stability tests of these data are examined to use the prediction process as unit root tests and estimation of coefficients (ACF & APCF). Phillips-Peron's and Dickey-Fuller's tests show that the data series is unstable at the level, which means that there is

a general trend in the series. As shown in Fig. 2. In this regard, we process the data by converting it to the logarithm and taking the first differences to remove the effect of the general trend from the series to be used in estimation and prediction, see Fig. 3. Furthermore, we repeat the unit root tests as in Table 3. Hence, we find that the calculated values are more significant than the critical values and Prob. = 0.0000, which is less than 5%, this indicates that the data series does not have a unit root and has become stable.

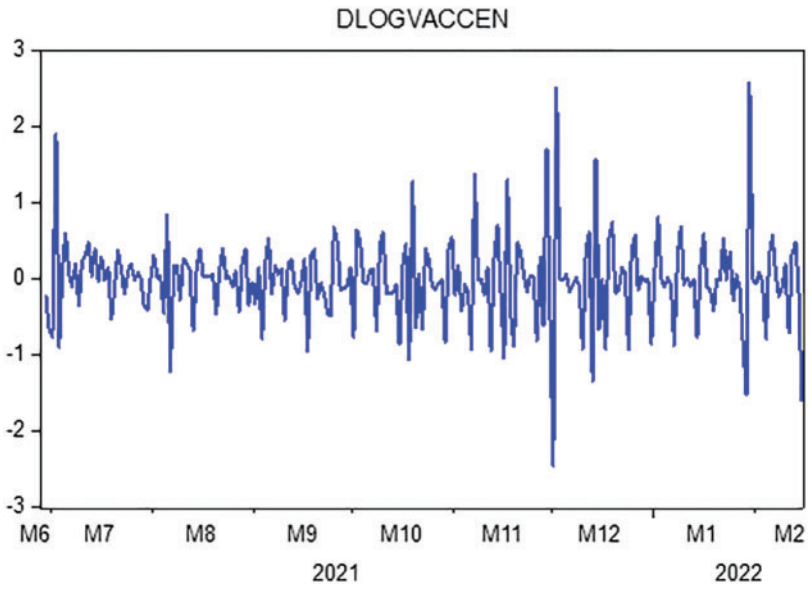

Figure 3: Transformation of the data of completely vaccinated people in KSA to the first difference

Table 3: Test statistic (Augmented Dickey-Fuller & Phillips-Perron)

			Test critical values		
Test statistic	t-statistic	Prob.	0.01	0.05	0.10
Augmented Dickey-Fuller	−6.293644	0.0000	−3.459362	−2.874200	−2.573594
Phillips-Perron	−25.09233	0.0000	−3.458594	−2.873863	−2.573413

We apply ARIMA models for forecasting through the Eviews program on the data series about the number of vaccinated people completely in KSA. As well, we estimate ARIMA models by using the Ordinary Least Squares method, as shown in Table 4. On the other hand, the models that have no statistical significance are excluded and the comparison only in the statistically significant models, and we are choosing a proper model that achieves the best models in which the coefficient of determination is greater, less variance, less volatility, and less value to AIC indicator.

Moreover, we check the ARIMA (1, 1, 2) model by testing residuals and the shape of the autocorrelation and partial autocorrelation coefficients. It follows from Fig. 4 that the actual values match the estimated values, and this indicates that the differences were small, as well as the efficiency of the model and its suitability in the forecasting process.

Table 4: Test result of ARIMA(p, d, q) models

MODELS	SIGMASQ	Adjusted R2	AIC	SC
ARIMA(1, 1, 1)	0.23	0.27	1.44	1.50
ARIMA(1, 1, 2)	0.23	0.28	1.43	1.49
ARIMA(1, 1, 7)	0.26	0.18	1.55	1.61
ARIMA(1, 1, 0)	0.29	0.11	1.63	1.67
ARIMA(0, 1, 1)	0.24	0.26	1.44	1.49
ARIMA(0, 1, 7)	0.31	0.05	1.71	1.74
ARIMA(2, 1, 0)	0.31	0.02	1.72	1.76
ARIMA(2, 1, 1)	0.23	0.27	1.43	1.49
ARIMA(2, 1, 7)	0.30	0.07	1.68	1.74
ARIMA(5, 1, 1)	0.23	0.27	1.44	1.50

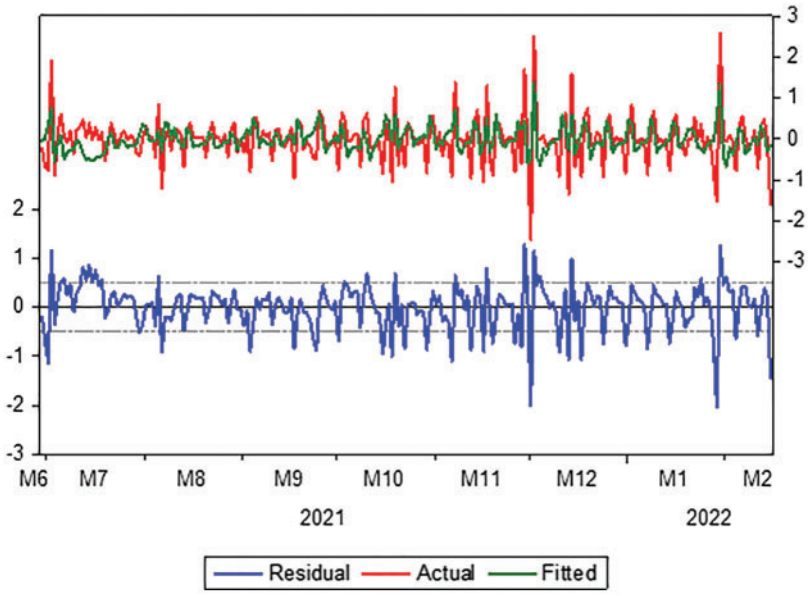

Figure 4: Evaluation of the ARIMA model for actual and fitted values and residual limits

We see through the chosen model a decrease in the number of people who will be fully dosed to (927164) during the predictive period from February 16, 2022, to April 14, 2022. For more details, see Fig. 5 and Table 6.

Finally, we estimate a linear model using the least-squares method to test the predictive ability of the model. Indeed, we take the actual values as a dependent variable and the estimated values as an independent variable. We conclude that the closer the estimated parameter to one, the more closely the estimated values are to the actual values. Through the results of Table 5, it is clear that the predicted parameter is close to one (0.955688), and this indicates the quality of the model in prediction and that there is a convergence of the predicted values from the actual values and is statistically significant.

Additionally, we find that the value of F = 1287.919, whereas Prob. = 0.0000 is less than 0.05, which indicates the model is significant and good.

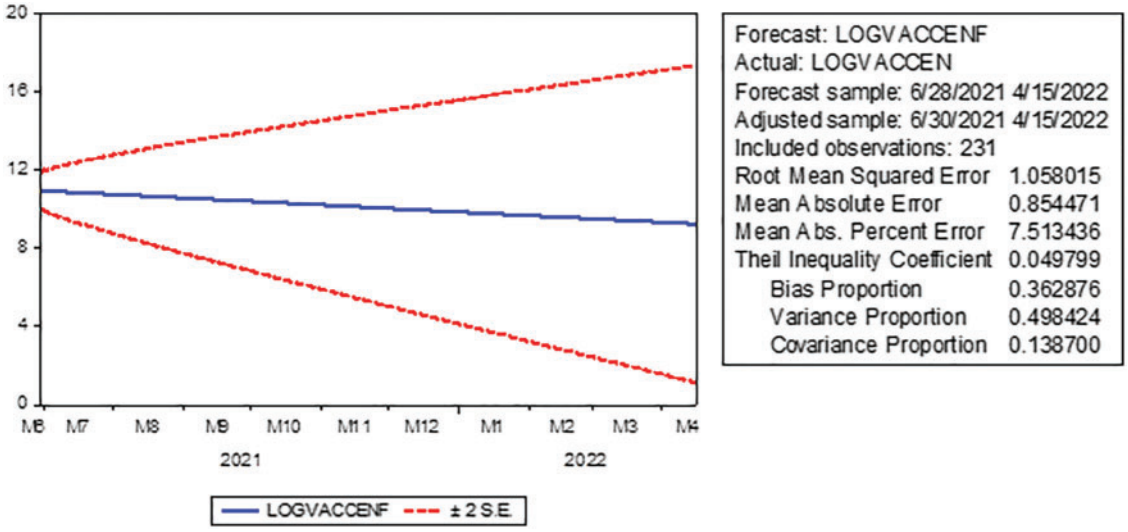

Figure 5: Prediction of the number of fully vaccinated people in KSA with confidence intervals (95%) for the period February 16, 2022 to April 15, 2022

Table 5: Test results of the predictive ability of a linear completed vaccinations in KSA

Dependent variable: Completed vaccinations Method: Least squares Included observations: 233				
Variable	Coefficient	Std. error	t-statistic	Prob.
PREDICTED	0.955688	0.018192	52.53	0.0000
R-squared	0.847083			
Adjusted R-squared	0.847083			
F	1287.919			
Prob.	0.000000			
Durbin-Watson stat	1.870376			

Table 6: Test results of the predictive ability of a linear completed vaccinations in KSA

Date	Forecast	UCL	LCL	Date	Forecast	UCL	LCL
2/16/2022	11344	26416	3832	3/18/2022	15432	62461	1611
2/17/2022	15750	38665	4865	3/19/2022	15504	63476	1568
2/18/2022	14055	34898	4257	3/20/2022	15577	64492	1526

(Continued)

Table 6 (continued)

Date	Forecast	UCL	LCL	Date	Forecast	UCL	LCL
2/19/2022	13295	33778	3867	3/21/2022	15650	65508	1485
2/20/2022	13558	35452	3745	3/22/2022	15724	66524	1446
2/21/2022	13769	36936	3629	3/23/2022	15797	67540	1408
2/22/2022	13812	37925	3485	3/24/2022	15872	68557	1372
2/23/2022	13851	38903	3348	3/25/2022	15946	69575	1337
2/24/2022	13918	39957	3223	3/26/2022	16021	70592	1303
2/25/2022	13987	41014	3107	3/27/2022	16096	71610	1270
2/26/2022	14053	42053	2997	3/28/2022	16172	72629	1238
2/27/2022	14118	43086	2892	3/29/2022	16248	73648	1207
2/28/2022	14184	44119	2792	3/30/2022	16324	74668	1178
3/1/2022	14251	45149	2698	3/31/2022	16400	75688	1149
3/2/2022	14318	46176	2609	4/1/2022	16477	76709	1121
3/3/2022	14385	47201	2524	4/2/2022	16555	77731	1094
3/4/2022	14453	48224	2442	4/3/2022	16632	78753	1067
3/5/2022	14520	49246	2365	4/4/2022	16711	79775	1042
3/6/2022	14589	50267	2291	4/5/2022	16789	80799	1017
3/7/2022	14657	51286	2220	4/6/2022	16868	81822	993
3/8/2022	14726	52304	2153	4/7/2022	16947	82847	970
3/9/2022	14795	53321	2088	4/8/2022	17026	83872	947
3/10/2022	14864	54338	2026	4/9/2022	17106	84898	926
3/11/2022	14934	55354	1967	4/10/2022	17187	85924	904
3/12/2022	15004	56370	1910	4/11/2022	17267	86951	884
3/13/2022	15075	57386	1855	4/12/2022	17348	86951	863
3/14/2022	15146	58401	1802	4/13/2022	17430	89007	844
3/15/2022	15217	59416	1752	4/14/2022	17512	90035	825
3/16/2022	15288	60431	1703	4/15/2022	17594	91065	807
3/17/2022	15360	61446	1656				

3 Auxiliary Results

Definition 3.1. [20] Let $\rho \in [0,1]$, and $\omega \in \mathscr{H}^1(a,b)$, $b > a$. Then, the ABC fractional derivative of order ρ is defined by

$$ {}^{ABC}\mathfrak{D}^{\rho}_{a^+}\omega(t) = \frac{\aleph(\rho)}{1-\rho}\int_a^t E_\rho\left(\frac{\rho}{\rho-1}(t-\theta)^\rho\right)\omega'(\theta)\,d\theta,\ t>0, \tag{1}$$

The normalization function $\aleph(\rho)$ satisfies $\aleph(0) = \aleph(1) = 1$, where E_ρ is the Mittag-Leffler function defined by

$$E_\rho(z) = \sum_{k=0}^{\infty}\frac{z^k}{\Gamma(k\rho+1)},\ \mathrm{Re}(\rho) > 0, z \in \mathbb{C}.$$

Definition 3.2. [20] The correspondent AB fractional integral is given by

$$^{AB}\Im^{\rho}_{a^+}\omega(t)=\frac{1-\rho}{\aleph(\rho)}\omega(t)+\frac{\rho}{\aleph(\rho)\Gamma(\rho)}\int_a^t(t-\theta)^{\rho-1}\omega(\theta)\,d\theta,\quad \rho\in[0,1].$$

Lemma 3.1. [22] Let $\omega(t)$ be a function defined on $[a,b]$ and $0<\rho\leq 1$. Then

$$^{ABABC}\Im^{\rho}_{a^+}\,{}^{ABC}\mathfrak{D}^{\rho}_{a^+}\omega(t)=\omega(t)-\omega(a).$$

Lemma 3.2. [20] The Laplace transform of the ABC fractional derivative is defined by

$$\mathcal{L}\,{}^{ABC}\mathfrak{D}^{\rho}_{0^+}\omega(t)=\frac{\aleph(\rho)}{1-\rho}\frac{s^{\rho}\mathcal{L}\{\omega(t)\}(s)-s^{\rho-1}\omega(0)}{s^{\rho}+\frac{\rho}{1-\rho}}.$$

Lemma 3.3. [20] The fractional differential system $^{ABC}\mathfrak{D}^{\rho}_{0^+}\omega(t)=f(t)$, $\omega(0)=\omega_0$, gives the unique solution

$$\omega(t)=\omega_0+\frac{1-\rho}{\aleph(\rho)}f(t)+\frac{\rho}{\aleph(\rho)\Gamma(\rho)}\int_a^t(t-\theta)^{\rho-1}f(\theta)\,d\theta,\quad \rho\in[0,1].$$

4 Model Derivation in ABC Operator

Yavuz et al. [41] developed a mathematical model to reveal the effects of vaccine treatment on COVID-19 described by a system of ODEs as follows:

$$\begin{cases}\dot{S}(\varkappa)=\Lambda-(\alpha\mathbf{E}(\varkappa)+m+\mu)\mathbf{S}(\varkappa),\\ \dot{\mathbf{E}}(\varkappa)=\alpha\mathbf{E}(\varkappa)\mathbf{S}(\varkappa)+p\mathbf{V}(\varkappa)\mathbf{E}(\varkappa)-(\kappa\mathbf{I}(\varkappa)+c+\mu)\mathbf{E}(\varkappa),\\ \dot{\mathbf{I}}(\varkappa)=\kappa\mathbf{I}(\varkappa)\mathbf{E}(\varkappa)-(z+\mu+\sigma)\mathbf{I}(\varkappa),\\ \dot{\mathbf{V}}(\varkappa)=m\mathbf{S}(\varkappa)-(p\mathbf{E}(\varkappa)+\mu)\mathbf{V}(\varkappa),\\ \dot{\mathbf{R}}(\varkappa)=z\mathbf{I}(\varkappa)+c\mathbf{E}(\varkappa)-\mu\mathbf{R}(\varkappa).\end{cases}\tag{2}$$

With initial conditions

$$\mathbf{S}(0)=\mathbf{S}_0,\mathbf{E}(0)=\mathbf{E}_0,\mathbf{I}(0)=\mathbf{I}_0,\mathbf{V}(0)=\mathbf{V}_0,\mathbf{R}(0)=\mathbf{R}_0.$$

In the present work, we make extend the model (2) by replacing the time derivative with the ABC fractional derivative. With this alteration, the right-and left-hand sides will not have the same dimensions. To conquer this affair, we add an auxiliary parameter $\mathscr{K}$ with the dimension of s, to change the nonlocal fractional operator so that the sides possess the same dimension [43]. Herewith, we reformulate the following fractional system:

$$\begin{cases}\frac{1}{\mathscr{K}^{1-\Theta}}\,{}^{ABC}\mathfrak{D}^{\Theta}\mathbf{S}(\varkappa)=\Lambda-(\alpha\mathbf{E}(\varkappa)+m+\mu)\mathbf{S}(\varkappa),\\ \frac{1}{\mathscr{K}^{1-\Theta}}\,{}^{ABC}\mathfrak{D}^{\Theta}\mathbf{E}(\varkappa)=\alpha\mathbf{E}(\varkappa)\mathbf{S}(\varkappa)+p\mathbf{V}(\varkappa)\mathbf{E}(\varkappa)-(\kappa\mathbf{I}(\varkappa)+c+\mu)\mathbf{E}(\varkappa),\\ \frac{1}{\mathscr{K}^{1-\Theta}}\,{}^{ABC}\mathfrak{D}^{\Theta}\mathbf{I}(\varkappa)=\kappa\mathbf{I}(\varkappa)\mathbf{E}(\varkappa)-(z+\mu+\sigma)\mathbf{I}(\varkappa),\\ \frac{1}{\mathscr{K}^{1-\Theta}}\,{}^{ABC}\mathfrak{D}^{\Theta}\mathbf{V}(\varkappa)=m\mathbf{S}(\varkappa)-(p\mathbf{E}(\varkappa)+\mu)\mathbf{V}(\varkappa),\\ \frac{1}{\mathscr{K}^{1-\Theta}}\,{}^{ABC}\mathfrak{D}^{\Theta}\mathbf{R}(\varkappa)=z\mathbf{I}(\varkappa)+c\mathbf{E}(\varkappa)-\mu\mathbf{R}(\varkappa).\end{cases}\tag{3}$$

With initial conditions

$$\mathbf{S}(0) = \mathbf{S}_0 \geq 0, \mathbf{E}(0) = \mathbf{E}_0 \geq 0, \mathbf{I}(0) = \mathbf{I}_0 \geq 0, \mathbf{V}(0) = \mathbf{V}_0 \geq 0, \mathbf{R}(0) = \mathbf{R}_0 \geq 0, \tag{4}$$

where ${}^{ABC}\mathfrak{D}^{\Theta}$ is the ABC fractional derivative of order $\Theta \in (0, 1]$, the functions $S(\varkappa)$, $E(\varkappa)$, $I(\varkappa)$, $V(\varkappa)$, $R(\varkappa)$ and their fractional derivatives are continuous at $\varkappa \geq 0$, and $(\mathbf{S}, \mathbf{E}, \mathbf{I}, \mathbf{V}, \mathbf{R}) \in \Lambda^5$, where $\Lambda := \mathscr{C}([0, T], \mathbb{R})$ is a Banach space endowed with the norm $\|\mathcal{X}\| := \sup_{t\in[0,T]} \{|\mathcal{X}(t)|\}$. Furthermore, we set $\Omega := (\Lambda^5, \|\mathcal{X}\|)$ with the norm $||\mathcal{X}|| = ||\mathbf{S}|| + ||\mathbf{E}|| + ||\mathbf{I}|| + ||\mathbf{V}|| + ||\mathbf{R}||$.

Here $S(\varkappa)$ is the class of Susceptible Individuals, $E(\varkappa)$ is the class of Exposed Individuals, $I(\varkappa)$ is the class of Infected individuals, $V(\varkappa)$ is the class of Individuals Vaccinated, $R(\varkappa)$ is the class of Recovered Individuals. The model parameter values and source are given in Table 7.

Total population at time $\varkappa$, denoted by $N(\varkappa)$ and given by $N(\varkappa) = S(\varkappa) + E(\varkappa) + I(\varkappa) + V(\varkappa) + R(\varkappa)$.

Table 7: Description of parameters and numerical values of the models (3) and (4)

Parameter	Description	Numerical value	Source
Λ	Rate of transmission from all individuals to individuals sensitive to the disease	0.999	Assumed
α	Rate of transmission from susceptible individuals to individuals who are exposed to the disease	0.002	[41]
m	Rate of exposure and those who have not been exposed to the disease are passed on to individuals to be vaccinated	0.4	Estimated
p	Rate of vaccinated individuals and their likelihood of contracting the disease due to vaccine failure	0.0001	Estimated
κ	Transmission rate from symptomatic individuals to the active patient portion	0.008	[41]
c	The rate of people recovering without symptoms and moving to the recovery part	0.005	Assumed
σ	Deaths rate among active patients	0.08	[41]
z	Recovery rate depending on the disease	0.012	[41]
μ	Natural deaths rate in all compartments	0.009	[41]
$\mathbf{S}_0$	Initial susceptible population	9,317,558	Assumed
$\mathbf{E}_0$	Initial exposed population	0	Assumed
$\mathbf{I}_0$	Initial infected population	562,300	Assumed
$\mathbf{V}_0$	Initial vaccinated population	24,000,000	Estimated
$\mathbf{R}_0$	Initial recovered population	580,000	Estimated

4.1 Positivity and Boundedness

In this portion, we show that the non-negative domain $\mathbb{R}^5$ is positively invariant region and the solutions of model are bounded, where $\mathbb{R}^5_+ = \{\Phi \in \mathbb{R}^5 : \Phi(\varkappa) \geq 0\}$.

Theorem 4.1. There is a unique solution $\Phi(\varkappa) = (\mathbf{S}(\varkappa), \mathbf{E}(\varkappa), \mathbf{I}(\varkappa), \mathbf{V}(\varkappa), \mathbf{R}(\varkappa))^T$ for the models (3) and (4) on $\varkappa \geq 0$ in $[0, T]$ $(0 < T < \infty)$ and the solution will remain in $\mathbb{R}^5$. Furthermore, the solution is stated in the region $\Delta \subset \mathbb{R}^5_+$, described by

$$\Delta = \left\{ (\mathbf{S}(\varkappa), \mathbf{E}(\varkappa), \mathbf{I}(\varkappa), \mathbf{V}(\varkappa), \mathbf{R}(\varkappa)) \in \mathbb{R}^5 : \mathbf{N}(\varkappa) \leq \frac{\Lambda}{\mu} \right\}.$$

Proof. From the model (3), we have

$$\begin{aligned}
{}^{ABC}\mathfrak{D}^{\Theta}\mathbf{S}(\varkappa) &= \mathscr{K}^{1-\Theta}(\Lambda - (\alpha\mathbf{E}(\varkappa) + m + \mu)\mathbf{S}(\varkappa)),\\
{}^{ABC}\mathfrak{D}^{\Theta}\mathbf{E}(\varkappa) &= \mathscr{K}^{1-\Theta}(\alpha\mathbf{E}(\varkappa)\mathbf{S}(\varkappa) + p\mathbf{V}(\varkappa)\mathbf{E}(\varkappa) - (\kappa\mathbf{I}(\varkappa) + c + \mu)\mathbf{E}(\varkappa)),\\
{}^{ABC}\mathfrak{D}^{\Theta}\mathbf{I}(\varkappa) &= \mathscr{K}^{1-\Theta}(\kappa\mathbf{I}(\varkappa)\mathbf{E}(\varkappa) - (z + \mu + \sigma)\mathbf{I}(\varkappa)).\\
{}^{ABC}\mathfrak{D}^{\Theta}\mathbf{V}(\varkappa) &= \mathscr{K}^{1-\Theta}(m\mathbf{S}(\varkappa) - (p\mathbf{E}(\varkappa) + \mu)\mathbf{V}(\varkappa)).\\
{}^{ABC}\mathfrak{D}^{\Theta}\mathbf{R}(\varkappa) &= \mathscr{K}^{1-\Theta}(z\mathbf{I}(\varkappa) + c\mathbf{E}(\varkappa) - \mu\mathbf{R}(\varkappa)).
\end{aligned}$$

The norm and all assumptions of the classical results are valid. It follows that:

$$\begin{cases}
{}^{ABC}\mathfrak{D}^{\Theta}\mathbf{S}(\varkappa) \geq -\mathscr{K}^{1-\Theta}(\alpha\mathbf{E}(\varkappa) + m + \mu)\mathbf{S}(\varkappa),\\
{}^{ABC}\mathfrak{D}^{\Theta}\mathbf{E}(\varkappa) \geq -\mathscr{K}^{1-\Theta}(\kappa\mathbf{I}(\varkappa) + c + \mu)\mathbf{E}(\varkappa),\\
{}^{ABC}\mathfrak{D}^{\Theta}\mathbf{I}(\varkappa) \geq -\mathscr{K}^{1-\Theta}(z + \mu + \sigma)\mathbf{I}(\varkappa)\\
{}^{ABC}\mathfrak{D}^{\Theta}\mathbf{V}(\varkappa) \geq -\mathscr{K}^{1-\Theta}(p\mathbf{E}(\varkappa) + \mu)\mathbf{V}(\varkappa)\\
{}^{ABC}\mathfrak{D}^{\Theta}\mathbf{R}(\varkappa) \geq -\mathscr{K}^{1-\Theta}\mu\mathbf{R}(\varkappa)
\end{cases}$$

For $\mathscr{K} > 0$ and $\varkappa > 0$, we have

$$\begin{cases}
\mathbf{S}(\varkappa) \geq \mathbf{S}_0 E_{\Theta}\left(-\dfrac{\Theta\mathscr{K}^{1-\Theta}(\alpha\,||\mathbf{E}|| + m + \mu)\varkappa^{\Theta}}{\aleph(\Theta) - (1-\Theta)\mathscr{K}^{1-\Theta}(\alpha\,||\mathbf{E}|| + m + \mu)}\right),\\
\mathbf{E}(\varkappa) \geq \mathbf{E}_0 E_{\Theta}\left(-\dfrac{\Theta\mathscr{K}^{1-\Theta}(\kappa\,||\mathbf{I}|| + c + \mu)\varkappa^{\Theta}}{\aleph(\Theta) - (1-\Theta)\mathscr{K}^{1-\Theta}(\kappa\,||\mathbf{I}|| + c + \mu)}\right),\\
\mathbf{I}(\varkappa) \geq \mathbf{I}_0 E_{\Theta}\left(-\dfrac{\Theta\mathscr{K}^{1-\Theta}(z + \mu + \sigma)\varkappa^{\Theta}}{\aleph(\Theta) - (1-\Theta)\mathscr{K}^{1-\Theta}(z + \mu + \sigma)}\right),\\
\mathbf{V}(\varkappa) \geq \mathbf{V}_0 E_{\Theta}\left(-\dfrac{\Theta\mathscr{K}^{1-\Theta}(p\,||\mathbf{E}|| + \mu)\varkappa^{\Theta}}{\aleph(\Theta) - (1-\Theta)\mathscr{K}^{1-\Theta}(p\,||\mathbf{E}|| + \mu)}\right)\\
\mathbf{R}(\varkappa) \geq \mathbf{R}_0 E_{\Theta}\left(-\dfrac{\Theta\mathscr{K}^{1-\Theta}\mu\varkappa^{\Theta}}{\aleph(\Theta) - (1-\Theta)\mathscr{K}^{1-\Theta}\mu}\right).
\end{cases}$$

This shows that if $\mathbf{S}_0, \mathbf{E}_0, \mathbf{I}_0, \mathbf{V}_0$, and $\mathbf{R}_0$ are positive, then $\mathrm{S}(\varkappa)$, $\mathrm{E}(\varkappa)$, $\mathrm{I}(\varkappa)$, $\mathrm{V}(\varkappa)$, and $\mathrm{R}(\varkappa)$ are also positive. Now, we give a biologically feasible region for the suggested models (3) and (4). Consider summing all the equations in the model as follows

$$\frac{1}{\mathscr{K}^{1-\Theta}}{}^{ABC}\mathfrak{D}^{\Theta}\mathbf{N}(\varkappa) = \frac{1}{\mathscr{K}^{1-\Theta}}{}^{ABC}\mathfrak{D}^{\Theta}(\mathbf{S}(\varkappa) + \mathbf{E}(\varkappa) + \mathbf{I}(\varkappa) + \mathbf{V}(\varkappa) + \mathbf{R}(\varkappa)).$$

It follows for the whole population that

$$\begin{aligned}
{}^{ABC}\mathfrak{D}^{\Theta}\mathbf{N}(\varkappa) &= \mathscr{K}^{1-\Theta}(\Lambda - \mu\mathbf{N}(\varkappa) - \sigma\mathbf{I}(\varkappa))\\
&\leq \mathscr{K}^{1-\Theta}(\Lambda - \mu\mathbf{N}(\varkappa)),
\end{aligned}$$

which implies that

$${}^{ABC}\mathfrak{D}^{\Theta}\mathbf{N}(\varkappa) \leq \mathscr{K}^{1-\Theta}(\Lambda - \mu\mathbf{N}(\varkappa)).$$

After applying the Laplace transform, we have

$$\mathbf{N}(s) \leq \left(\frac{\mathscr{K}^{1-\Theta}(1-\Theta)\Lambda}{\vartheta} + \frac{\aleph(\Theta)}{\vartheta}\mathbf{N}(0)\right)\frac{s^{\Theta-1}}{(s^{\Theta}+\lambda)} + \frac{\mathscr{K}^{1-\Theta}\Theta\Lambda}{\vartheta}\frac{s^{-1}}{(s^{\Theta}+\lambda)},$$

where $\vartheta := [\aleph(\Theta) + \mathscr{K}^{1-\Theta}(1-\Theta)\mu]$, and $\lambda = \dfrac{\mathscr{K}^{1-\Theta}\Theta\mu}{[\aleph(\Theta) + \mathscr{K}^{1-\Theta}(1-\Theta)\mu]}$. Using the inverse Laplace, we get

$$\mathbf{N}(\varkappa) = \left(\frac{\mathscr{K}^{1-\Theta}(1-\Theta)\Lambda}{\vartheta} + \frac{\aleph(\Theta)\mathbf{N}(0)}{\vartheta}\right)E_{\Theta,1}\left(-\lambda\varkappa^{\Theta}\right) + \frac{\mathscr{K}^{1-\Theta}\Theta\Lambda}{\vartheta}\varkappa^{\Theta}E_{\Theta,\Theta+1}\left(-\lambda\varkappa^{\Theta}\right),$$

where $E_{\alpha,\beta}(z) = \sum_{k=0}^{\infty}\dfrac{z^k}{\Gamma(k\alpha+\beta)}$, and $\mathcal{L}\left[\varkappa^{\beta-1}E_{\alpha,\beta}(\pm a\varkappa^{\alpha})\right] = \dfrac{s^{\alpha-\beta}}{(s^{\alpha}\mp a)}$. Subsequently, the solution of the model with the nonnegative conditions in Δ stays in Δ. In this way, the region Δ is positively invariant and attracts all the solutions in $\mathbb{R}^5$. This shows that the models (3) and (4) is epidemiologically well posed and the solutions.

4.2 Equilibrium Points and Reproduction Number

In this part, we will find the equilibrium points of the COVID-19 model. By equating each equation of model (3) to the zero, we can write

$$\begin{aligned}
0 &= \mathscr{K}^{1-\Theta}(\Lambda - (\alpha\mathbf{E} + m + \mu)\mathbf{S}),\\
0 &= \mathscr{K}^{1-\Theta}(\alpha\mathbf{E}\mathbf{S} + p\mathbf{V}\mathbf{E} - (\kappa\mathbf{I} + c + \mu)\mathbf{E}),\\
0 &= \mathscr{K}^{1-\Theta}(\kappa\mathbf{I}\mathbf{E} - (z + \mu + \sigma)\mathbf{I}).\\
0 &= \mathscr{K}^{1-\Theta}(m\mathbf{S} - (p\mathbf{E} + \mu)\mathbf{V}).\\
0 &= \mathscr{K}^{1-\Theta}(z\mathbf{I} + c\mathbf{E} - \mu\mathbf{R}).
\end{aligned}$$

For $\mathscr{K} > 0$, we have

$$\begin{aligned}
0 &= \Lambda - (\alpha\mathbf{E} + m + \mu)\mathbf{S},\\
0 &= \alpha\mathbf{E}\mathbf{S} + p\mathbf{V}\mathbf{E} - (\kappa\mathbf{I} + c + \mu)\mathbf{E},\\
0 &= \kappa\mathbf{I}\mathbf{E} - (z + \mu + \sigma)\mathbf{I}.\\
0 &= m\mathbf{S} - (p\mathbf{E} + \mu)\mathbf{V}.\\
0 &= z\mathbf{I} + c\mathbf{E} - \mu\mathbf{R}.
\end{aligned}$$

Hence, the disease free equilibrium (DFE) and endemic equilibrium (EE) are given by the following theorem.

Theorem 4.2. We have the next affirmations:

i. The model (3) has always DFE, $\mathbb{E}_0 = (\mathbf{S}_0, \mathbf{E}_0, \mathbf{I}_0, \mathbf{V}_0, \mathbf{R}_0)$, where $\mathbf{S}_0 = \dfrac{\Lambda}{m+\mu}$, $\mathbf{E}_0 = 0$, $\mathbf{I}_0 = 0, \mathbf{V}_0 = \dfrac{\Lambda m}{(m+\mu)\mu}$, and $\mathbf{R}_0 = 0$.

ii. The model (3) has EE, $\mathbb{E}^* = (\mathbf{S}^*, \mathbf{E}^*, \mathbf{I}^*, \mathbf{V}^*, \mathbf{R}^*)$, where

$$\mathbf{S}^* = \frac{\kappa\Lambda}{\alpha\mu + \alpha\sigma + \kappa\mu + \kappa m + \alpha z}$$

$$\mathbf{E}^* = \frac{\sigma + \mu + z}{\kappa}$$

$$\mathbf{I}^* = \frac{\kappa\left(\Lambda\left(\alpha\mu + mp\right) + \alpha p(\sigma + \mu + z)\right)}{\left(\kappa\mu + p\sigma + p\mu + pz\right)\left(\kappa m + \kappa\mu + \alpha\sigma + \alpha\mu + \alpha z\right)} - \frac{c + \mu}{\kappa}$$

$$\mathbf{V}^* = \frac{\kappa^2 \Lambda m}{\left(\kappa\mu + p\sigma + p\mu + pz\right)\left(\kappa m + \kappa\mu + \alpha\sigma + \alpha\mu + \alpha z\right)}$$

$$\mathbf{R}^* = \frac{\kappa^2\left(m\left(\mu\left(c\left(\mu + \sigma\right) - \mu z\right) + \Lambda p z\right) + \mu\left(c\mu\left(\mu + \sigma\right) + z\left(\alpha\Lambda - \mu^2\right)\right)\right)}{\kappa\mu\left(\kappa\mu + p\sigma + p\mu + pz\right)\left(\kappa m + \kappa\mu + \alpha\sigma + \alpha\mu + \alpha z\right)}$$
$$+ \frac{\kappa\left(\mu + \sigma + z\right) + p\left(c\left(\mu + \sigma\right)\left(\mu + m\right) + z\left(\alpha\Lambda - \mu\left(\mu + m\right)\right)\right)}{\kappa\mu\left(\kappa\mu + p\sigma + p\mu + pz\right)\left(\kappa m + \kappa\mu + \alpha\sigma + \alpha\mu + \alpha z\right)}$$
$$+ \frac{\alpha\mu(c(\mu + \sigma) - \mu z) + \alpha p(\sigma + \mu + z)^2(c(\mu + \sigma) - \mu z)}{\kappa\mu\left(\kappa\mu + p\sigma + p\mu + pz\right)\left(\kappa m + \kappa\mu + \alpha\sigma + \alpha\mu + \alpha z\right)}.$$

By using the model (3) and next generation matrix method, the basic reproduction number R_0 calculated as

$$R_0 = \frac{\Lambda(\mu\alpha + mp)}{\mu(\mu + c)(\mu + m)}.$$

For details, see [41].

4.3 Stability Analysis

Stability analysis of the equilibrium points is clarified in [41], exhaustively. In order of stability, the authors dealt with the next two theorems.

Theorem 4.3. The DFE point $\mathbb{E}_0$ of the epidemic model is locally asymptotically stable if $R_0 < 1$, otherwise unstable.

Theorem 4.4. The EE point $\mathbb{E}^*$ of the epidemic model is locally asymptotically stable if $R_0 > 1$, otherwise unstable.

Here we comment that R_0 gives us data about the transmission of infectious sickness. For example in the normal utilization of contamination models, when $R_0 > 1$, the disease infection will actually be able to begin transmitting in society, yet if $R_0 < 1$ it implies that the disease infection continues declining in the general public. Overall, the bigger the worth of R_0 the troublesome it is to control the pandemic from spreading in the public arena.

5 Existence Criteria

In this section, we apply the Picard-Lindel method and the Laplace transform to investigate the existence and uniqueness of solution for preventive and curative to fractional COVID-19 disease model.

5.1 Iterative Scheme with Laplace Transform

Theorem 5.1. For $0 < \Theta \leq 1$, the following ABC-type FDE

$$\frac{1}{\mathscr{K}^{1-\alpha}}{}^{ABC}\mathfrak{D}^{\Theta}\mathbf{u}\left(\varkappa\right) = \mathbf{f}\left(\varkappa\right) \tag{5}$$

has a unique solution, which is

$$\mathbf{u}(\varkappa)=\mathbf{u}(0)+\frac{(1-\Theta)\kappa^{1-\Theta}}{\aleph(\Theta)}\mathbf{f}(\varkappa)+\frac{\Theta\kappa^{1-\Theta}}{\aleph(\Theta)\Gamma(\Theta)}\int_0^{\varkappa}(\varkappa-\nu)^{\Theta-1}\mathbf{f}(\nu)\,d\nu. \tag{6}$$

Proof. Applying the Laplace transform on both sides of Eq. (5) we obtain

$$\mathcal{L}\left\{\frac{1}{\mathscr{K}^{1-\Theta}}{}^{ABC}\mathfrak{D}^{\Theta}\mathbf{u}(\varkappa)\right\}(\varpi)=\mathcal{L}\{\mathbf{f}(\varkappa)\}(\varpi),\ \varpi>0.$$

It follows from Theorem 3 in [20] that

$$\frac{\aleph(\Theta)}{1-\Theta}\frac{\varpi^{\Theta}\mathcal{L}(\mathbf{u}(\varkappa))(\varpi)-\varpi^{\Theta-1}\mathbf{u}(0)}{\varpi^{\Theta}+\frac{\Theta}{1-\Theta}}=\mathscr{K}^{1-\Theta}\mathcal{L}\{\mathbf{f}(\varkappa)\}(\varpi),$$

which is equivalent to

$$\mathcal{L}(\mathbf{u}(\varkappa))(\varpi)=\frac{1}{\varpi}\mathbf{u}(0)+\frac{(1-\Theta)\mathscr{K}^{1-\Theta}}{\aleph(\Theta)}\mathcal{L}\{\mathbf{f}(\varkappa)\}(\varpi)+\frac{\Theta\mathscr{K}^{1-\Theta}}{\varpi^{\Theta}\aleph(\Theta)}\mathcal{L}\{\mathbf{f}(\varkappa)\}(\varpi).$$

Applying the inverse Laplace transform give us

$$\mathbf{u}(\varkappa)=\mathbf{u}(0)+\frac{(1-\Theta)\mathscr{K}^{1-\Theta}}{\aleph(\Theta)}\mathbf{f}(\varkappa)+\mathcal{L}^{-1}\left\{\frac{\Theta\mathscr{K}^{1-\Theta}}{\varpi^{\Theta}\aleph(\Theta)}\mathcal{L}\{\mathbf{f}(\varkappa)\}(\varpi)\right\}(\varkappa).$$

Now, we have

$$\frac{\Theta\mathscr{K}^{1-\Theta}}{\aleph(\Theta)}\left(\frac{1}{\varpi^{\Theta}}\right)=\frac{\Theta\mathscr{K}^{1-\Theta}}{\aleph(\Theta)}\mathcal{L}\left\{\frac{\varkappa^{\Theta-1}}{\Gamma(\Theta)}\right\}(\varpi).$$

Let $\mathbf{F}(\varpi)=\frac{\Theta\mathscr{K}^{1-\Theta}}{\aleph(\Theta)}\mathcal{L}\left\{\frac{\varkappa^{\Theta-1}}{\Gamma(\Theta)}\right\}(\varpi)$, and $\mathbf{G}(\varpi)=\mathcal{L}\{\mathbf{f}(\varkappa)\}(\varpi)$. It follows form convolution theorem that

$$\begin{aligned}\mathcal{L}^{-1}\left\{\frac{\Theta\mathscr{K}^{1-\Theta}}{\varpi^{\Theta}\aleph(\Theta)}\mathcal{L}\{\mathbf{f}(\varkappa)\}(\varpi)\right\}(\varkappa)&=\mathcal{L}^{-1}\{\mathbf{F}(\varpi)\times\mathbf{G}(\varpi)\}(\varkappa)\\&=\frac{\Theta\mathscr{K}^{1-\Theta}}{\aleph(\Theta)}\left\{\frac{\varkappa^{\Theta-1}}{\Gamma(\Theta)}*\mathbf{f}(\varkappa)\right\}(\varpi)\\&=\frac{\Theta\mathscr{K}^{1-\Theta}}{\aleph(\Theta)\Gamma(\Theta)}\int_0^{\varkappa}(\varkappa-\varpi)^{\Theta-1}\mathbf{f}(\varpi)\,d\varpi.\end{aligned}$$

Hence

$$\mathbf{u}(\varkappa)=\mathbf{u}(0)+\frac{(1-\Theta)\mathscr{K}^{1-\Theta}}{\aleph(\Theta)}\mathbf{f}(\varkappa)+\frac{\Theta\mathscr{K}^{1-\Theta}}{\aleph(\Theta)\Gamma(\Theta)}\int_0^{\varkappa}(\varkappa-\nu)^{\Theta-1}\mathbf{f}(\nu)\,d\nu.$$

By using Theorem 5.1, our model is equivalent to

$$\begin{cases}
\mathbf{S}(\varkappa)-\mathbf{S}(0)=\dfrac{(1-\Theta)\mathscr{K}^{1-\Theta}}{\aleph(\Theta)}\{\Lambda-(\alpha\mathbf{E}(\varkappa)+m+\mu)\mathbf{S}(\varkappa)\}\\
+\dfrac{\Theta\mathscr{K}^{1-\Theta}}{\aleph(\Theta)\Gamma(\Theta)}\int_0^{\varkappa}(\varkappa-r)^{\Theta-1}\{\Lambda-(\alpha\mathbf{E}(r)+m+\mu)\mathbf{S}(r)\}dr\\
\mathbf{E}(\varkappa)-\mathbf{E}(0)=\dfrac{(1-\Theta)\mathscr{K}^{1-\Theta}}{\aleph(\Theta)}\{\alpha\mathbf{E}(\varkappa)\mathbf{S}(\varkappa)+p\mathbf{V}(\varkappa)\mathbf{E}(\varkappa)-(\kappa\mathbf{I}(\varkappa)+c+\mu)\mathbf{E}(\varkappa)\}\\
+\dfrac{\Theta\mathscr{K}^{1-\Theta}}{\aleph(\Theta)\Gamma(\Theta)}\int_0^{\varkappa}(\varkappa-r)^{\Theta-1}\{\alpha\mathbf{E}(r)\mathbf{S}(r)+p\mathbf{V}(r)\mathbf{E}(r)-(\kappa\mathbf{I}(r)+c+\mu)\mathbf{E}(r)\}dr\\
\mathbf{I}(\varkappa)-\mathbf{I}(0)=\dfrac{(1-\Theta)\mathscr{K}^{1-\Theta}}{\aleph(\Theta)}\{\kappa\mathbf{I}(\varkappa)\mathbf{E}(\varkappa)-(z+\mu+\sigma)\mathbf{I}(\varkappa)\}\\
+\dfrac{\Theta\mathscr{K}^{1-\Theta}}{\aleph(\Theta)\Gamma(\Theta)}\int_0^{\varkappa}(\varkappa-r)^{\Theta-1}\{\kappa\mathbf{I}(r)\mathbf{E}(r)-(z+\mu+\sigma)\mathbf{I}(r)\}dr\\
\mathbf{V}(\varkappa)-\mathbf{V}(0)=\dfrac{(1-\Theta)\mathscr{K}^{1-\Theta}}{\aleph(\Theta)}\{m\mathbf{S}(\varkappa)-(p\mathbf{E}(\varkappa)+\mu)\mathbf{V}(\varkappa)\}\\
+\dfrac{\Theta\mathscr{K}^{1-\Theta}}{\aleph(\Theta)\Gamma(\Theta)}\int_0^{\varkappa}(\varkappa-r)^{\Theta-1}\{m\mathbf{S}(r)-(p\mathbf{E}(r)+\mu)\mathbf{V}(r)\}dr\\
\mathbf{R}(\varkappa)-\mathbf{R}(0)=\dfrac{(1-\Theta)\mathscr{K}^{1-\Theta}}{\aleph(\Theta)}\{z\mathbf{I}(\varkappa)+c\mathbf{E}(\varkappa)-\mu\mathbf{R}(\varkappa)\}\\
+\dfrac{\Theta\mathscr{K}^{1-\Theta}}{\aleph(\Theta)\Gamma(\Theta)}\int_0^{\varkappa}(\varkappa-r)^{\Theta-1}\{z\mathbf{I}(r)+c\mathbf{E}(r)-\mu\mathbf{R}(r)\}dr
\end{cases}\tag{7}$$

The iterative scheme of the model (7) is given by

$$\mathbf{S}_0(\varkappa)=\mathbf{S}(0),\mathbf{E}_0(\varkappa)=\mathbf{E}(0),\ \mathbf{I}_0(\varkappa)=\mathbf{I}(0),\mathbf{V}_0(\varkappa)=\mathbf{V}(0),\ \mathbf{R}_0(\varkappa)=\mathbf{R}(0).$$

$$\begin{cases}
\mathbf{S}_{n+1}(\varkappa)=\dfrac{(1-\Theta)\mathscr{K}^{1-\Theta}}{\aleph(\Theta)}\{\Lambda-(\alpha\mathbf{E}_n(\varkappa)+m+\mu)\mathbf{S}_n(\varkappa)\}\\
+\dfrac{\Theta\mathscr{K}^{1-\Theta}}{\aleph(\Theta)\Gamma(\Theta)}\int_0^{\varkappa}(\varkappa-r)^{\Theta-1}\{\Lambda-(\alpha\mathbf{E}_n(r)+m+\mu)\mathbf{S}_n(r)\}dr\\
\mathbf{E}_{n+1}(\varkappa)=\dfrac{(1-\Theta)\mathscr{K}^{1-\Theta}}{\aleph(\Theta)}\{\alpha\mathbf{E}_n(\varkappa)\mathbf{S}_n(\varkappa)+p\mathbf{V}_n(\varkappa)\mathbf{E}_n(\varkappa)-(\kappa\mathbf{I}_n(\varkappa)+c+\mu)\mathbf{E}_n(\varkappa)\}\\
+\dfrac{\Theta\mathscr{K}^{1-\Theta}}{\aleph(\Theta)\Gamma(\Theta)}\int_0^{\varkappa}(\varkappa-r)^{\Theta-1}\{\alpha\mathbf{E}_n(r)\mathbf{S}_n(r)+p\mathbf{V}_n(r)\mathbf{E}_n(r)-(\kappa\mathbf{I}_n(r)+c+\mu)\mathbf{E}_n(r)\}dr\\
\mathbf{I}_{n+1}(\varkappa)=\dfrac{(1-\Theta)\mathscr{K}^{1-\Theta}}{\aleph(\Theta)}\{\kappa\mathbf{I}_n(\varkappa)\mathbf{E}_n(\varkappa)-(z+\mu+\sigma)\mathbf{I}_n(\varkappa)\}\\
+\dfrac{\Theta\mathscr{K}^{1-\Theta}}{\aleph(\Theta)\Gamma(\Theta)}\int_0^{\varkappa}(\varkappa-r)^{\Theta-1}\{\kappa\mathbf{I}_n(r)\mathbf{E}_n(r)-(z+\mu+\sigma)\mathbf{I}_n(r)\}dr\\
\mathbf{V}_{n+1}(\varkappa)=\dfrac{(1-\Theta)\mathscr{K}^{1-\Theta}}{\aleph(\Theta)}\{m\mathbf{S}_n(\varkappa)-(p\mathbf{E}_n(\varkappa)+\mu)\mathbf{V}_n(\varkappa)\}\\
+\dfrac{\Theta\mathscr{K}^{1-\Theta}}{\aleph(\Theta)\Gamma(\Theta)}\int_0^{\varkappa}(\varkappa-r)^{\Theta-1}\{m\mathbf{S}_n(r)-(p\mathbf{E}_n(r)+\mu)\mathbf{V}_n(r)\}dr\\
\mathbf{R}_{n+1}(\varkappa)=\dfrac{(1-\Theta)\mathscr{K}^{1-\Theta}}{\aleph(\Theta)}\{z\mathbf{I}_n(\varkappa)+c\mathbf{E}_n(\varkappa)-\mu\mathbf{R}_n(\varkappa)\}\\
+\dfrac{\Theta\mathscr{K}^{1-\Theta}}{\aleph(\Theta)\Gamma(\Theta)}\int_0^{\varkappa}(\varkappa-r)^{\Theta-1}\{z\mathbf{I}_n(r)+c\mathbf{E}_n(r)-\mu\mathbf{R}_n(r)\}dr
\end{cases}\tag{8}$$

Taking the limit as $n\to\infty$, we anticipate getting the exact solution.

5.2 Existence of a Unique Solution

In this portion, we apply the Picard-Lindel method to investigate the existence of solution for the fractional COVID-19 disease model, which its mathematical represente are presented by:

$$\begin{cases} \frac{1}{\mathscr{K}^{1-\Theta}}{}^{ABC}\mathfrak{D}^{\Theta}\mathbf{S}(\varkappa) = \Lambda - (\alpha\mathbf{E}(\varkappa) + m + \mu)\,\mathbf{S}(\varkappa), \\ \frac{1}{\mathscr{K}^{1-\Theta}}{}^{ABC}\mathfrak{D}^{\Theta}\mathbf{E}(\varkappa) = \alpha\mathbf{E}(\varkappa)\,\mathbf{S}(\varkappa) + p\mathbf{V}(\varkappa)\,\mathbf{E}(\varkappa) - (\kappa\mathbf{I}(\varkappa) + c + \mu)\,\mathbf{E}(\varkappa), \\ \frac{1}{\mathscr{K}^{1-\Theta}}{}^{ABC}\mathfrak{D}^{\Theta}\mathbf{I}(\varkappa) = \kappa\mathbf{I}(\varkappa)\,\mathbf{E}(\varkappa) - (z + \mu + \sigma)\,\mathbf{I}(\varkappa), \\ \frac{1}{\mathscr{K}^{1-\Theta}}{}^{ABC}\mathfrak{D}^{\Theta}\mathbf{V}(\varkappa) = m\mathbf{S}(\varkappa) - (p\mathbf{E}(\varkappa) + \mu)\,\mathbf{V}(\varkappa), \\ \frac{1}{\mathscr{K}^{1-\Theta}}{}^{ABC}\mathfrak{D}^{\Theta}\mathbf{R}(\varkappa) = z\mathbf{I}(\varkappa) + c\mathbf{E}(\varkappa) - \mu\mathbf{R}(\varkappa). \end{cases} \tag{9}$$

For sake of simpilicity, we define the functions Ψ_i, $i = 1, 2, \ldots, 5$, as follows:

$$\begin{cases} \Psi_1(\varkappa, \mathbf{S}(\varkappa)) = \Lambda - (\alpha\mathbf{E}(\varkappa) + m + \mu)\mathbf{S}(\varkappa), \\ \Psi_2(\varkappa, \mathbf{E}(\varkappa)) = \alpha\mathbf{E}(\varkappa)\mathbf{S}(\varkappa) + p\mathbf{V}(\varkappa)\mathbf{E}(\varkappa) - (\kappa\mathbf{I}(\varkappa) + c + \mu)\mathbf{E}(\varkappa), \\ \Psi_3(\varkappa, \mathbf{I}(\varkappa)) = \kappa\mathbf{I}(\varkappa)\mathbf{E}(\varkappa) - (z + \mu + \sigma)\mathbf{I}(\varkappa), \\ \Psi_4(\varkappa, \mathbf{V}(\varkappa)) = m\mathbf{S}(\varkappa) - (p\mathbf{E}(\varkappa) + \mu)\mathbf{V}(\varkappa), \\ \Psi_5(\varkappa, \mathbf{R}(\varkappa)) = z\mathbf{I}(\varkappa) + c\mathbf{E}(\varkappa) - \mu\mathbf{R}(\varkappa). \end{cases} \tag{10}$$

The model described in Eq. (9) becomes in the following form:

$$\begin{cases} \frac{1}{\mathscr{K}^{1-\Theta}}{}^{ABC}\mathfrak{D}^{\Theta}\mathbf{S}(\varkappa) = \Psi_1(\varkappa, \mathbf{S}(\varkappa)), \\ \frac{1}{\mathscr{K}^{1-\Theta}}{}^{ABC}\mathfrak{D}^{\Theta}\mathbf{E}(\varkappa) = \Psi_2(\varkappa, \mathbf{E}(\varkappa)), \\ \frac{1}{\mathscr{K}^{1-\Theta}}{}^{ABC}\mathfrak{D}^{\Theta}\mathbf{I}(\varkappa) = \Psi_3(\varkappa, \mathbf{I}(\varkappa)), \\ \frac{1}{\mathscr{K}^{1-\Theta}}{}^{ABC}\mathfrak{D}^{\Theta}\mathbf{V}(\varkappa) = \Psi_4(\varkappa, \mathbf{V}(\varkappa)), \\ \frac{1}{\mathscr{K}^{1-\Theta}}{}^{ABC}\mathfrak{D}^{\Theta}\mathbf{R}(\varkappa) = \Psi_5(\varkappa, \mathbf{R}(\varkappa)), \end{cases} \tag{11}$$

By applying the operator ${}^{AB}\Im^{\Theta}$ on Eq. (11), we obtain

$$\begin{cases} \mathbf{S}(\varkappa) - \mathbf{S}(0) = \frac{(1-\Theta)\mathscr{K}^{1-\Theta}}{\aleph(\Theta)}\Psi_1(\varkappa, \mathbf{S}(\varkappa)) + \frac{\Theta\mathscr{K}^{1-\Theta}}{\aleph(\Theta)\Gamma(\Theta)}\int_0^{\varkappa}(\varkappa - r)^{\Theta-1}\Psi_1(r, \mathbf{S}(r))\,dr, \\ \mathbf{E}(\varkappa) - \mathbf{E}(0) = \frac{(1-\Theta)\mathscr{K}^{1-\Theta}}{\aleph(\Theta)}\Psi_2(\varkappa, \mathbf{E}(\varkappa)) + \frac{\Theta\mathscr{K}^{1-\Theta}}{\aleph(\Theta)\Gamma(\Theta)}\int_0^{\varkappa}(\varkappa - r)^{\Theta-1}\Psi_2(r, \mathbf{E}(r))\,dr, \\ \mathbf{I}(\varkappa) - \mathbf{I}(0) = \frac{(1-\Theta)\mathscr{K}^{1-\Theta}}{\aleph(\Theta)}\Psi_3(\varkappa, \mathbf{I}(\varkappa)) + \frac{\Theta\mathscr{K}^{1-\Theta}}{\aleph(\Theta)\Gamma(\Theta)}\int_0^{\varkappa}(\varkappa - r)^{\Theta-1}\Psi_3(r, \mathbf{I}(r))\,dr, \\ \mathbf{V}(\varkappa) - \mathbf{V}(0) = \frac{(1-\Theta)\mathscr{K}^{1-\Theta}}{\aleph(\Theta)}\Psi_4(\varkappa, \mathbf{V}(\varkappa)) + \frac{\Theta\mathscr{K}^{1-\Theta}}{\aleph(\Theta)\Gamma(\Theta)}\int_0^{\varkappa}(\varkappa - r)^{\Theta-1}\Psi_4(r, \mathbf{V}(r))\,dr, \\ \mathbf{R}(\varkappa) - \mathbf{R}(0) = \frac{(1-\Theta)\mathscr{K}^{1-\Theta}}{\aleph(\Theta)}\Psi_5(\varkappa, \mathbf{R}(\varkappa)) + \frac{\Theta\mathscr{K}^{1-\Theta}}{\aleph(\Theta)\Gamma(\Theta)}\int_0^{\varkappa}(\varkappa - r)^{\Theta-1}\Psi_5(r, \mathbf{R}(r))\,dr. \end{cases} \tag{12}$$

The kernels in Eq. (10) satisfies the Lipschitz condition for $0 \leq L_i < 1$, $i = 1, 2, \ldots 5$, if and only if the nonlinear functions S($\varkappa$), E($\varkappa$), I($\varkappa$), V($\varkappa$) and R($\varkappa$) have an upper bound. Let S($\varkappa$) and $\mathbf{S}^{\star}(\varkappa)$ be

two functions. Then

$$\begin{aligned}||\Psi_1(\varkappa,\mathbf{S}(\varkappa))-\Psi_1(\varkappa,\mathbf{S}^{\star}(\varkappa))|| &= ||\Lambda-(\alpha\mathbf{E}(\varkappa)+m+\mu)\mathbf{S}(\varkappa)\\ &\quad -\Lambda+(\alpha\mathbf{E}(\varkappa)+m+\mu)\mathbf{S}^{\star}(\varkappa)||\\ &= ||(\alpha\mathbf{E}(\varkappa)+m+\mu)\left(\mathbf{S}^{\star}(\varkappa)-\mathbf{S}(\varkappa)\right)||\\ &\leq \left(\alpha\sup_{\varkappa\in[0,T]}\mathbf{E}(\varkappa)+m+\mu\right)||\mathbf{S}^{\star}(\varkappa)-\mathbf{S}(\varkappa)||\\ &= L_1||\mathbf{S}^{\star}(\varkappa)-\mathbf{S}(\varkappa)||, \end{aligned} \tag{13}$$

where $L_1:=\alpha\,||\mathbf{E}||+m+\mu$. Thus,

$$\left|\left|\Psi_1(\varkappa,\mathbf{S}(\varkappa))-\Psi_1(\varkappa,\mathbf{S}^{\star}(\varkappa))\right|\right|\leq L_1\left|\left|\mathbf{S}(\varkappa)-\mathbf{S}^{\star}(\varkappa)\right|\right|. \tag{14}$$

Repeating the same procedure as in Eq. (13), we get

$$\begin{aligned}||\Psi_2(\varkappa,\mathbf{E}(\varkappa))-\Psi_2(\varkappa,\mathbf{E}^{\star}(\varkappa))|| &\leq L_2\,||\mathbf{E}(\varkappa)-\mathbf{E}^{\star}(\varkappa)||,\\ ||\Psi_3(\varkappa,\mathbf{I}(\varkappa))-\Psi_3(\varkappa,\mathbf{I}^{\star}(\varkappa))|| &\leq L_3\,||\mathbf{I}(\varkappa)-\mathbf{I}^{\star}(\varkappa)||,\\ ||\Psi_4(\varkappa,\mathbf{V}(\varkappa))-\Psi_4(\varkappa,\mathbf{V}^{\star}(\varkappa))|| &\leq L_4\,||\mathbf{V}(\varkappa)-\mathbf{V}^{\star}(\varkappa)||,\\ ||\Psi_5(\varkappa,\mathbf{R}(\varkappa))-\Psi_5(\varkappa,\mathbf{R}^{\star}(\varkappa))|| &\leq L_5\,||\mathbf{R}(\varkappa)-\mathbf{R}^{\star}(\varkappa)||, \end{aligned} \tag{15}$$

where $L_2:=\alpha\,||\mathbf{S}||+p\,||\mathbf{V}||+\kappa\,||\mathbf{I}||+c+\mu$, $L_3:=\kappa\,||\mathbf{E}||+z+\mu+\sigma$, $L_4:=p\,||\mathbf{E}||+\mu$, and $L_5:=\mu$.

Eq. (12) can be written in the recursive form given by

$$\begin{cases} S_n(\varkappa)=\mathbf{S}(0)+\dfrac{(1-\Theta)\mathscr{K}^{1-\Theta}}{\aleph(\Theta)}\Psi_1(\varkappa,\mathbf{S}_{n-1}(\varkappa))+\dfrac{\Theta\mathscr{K}^{1-\Theta}}{\aleph(\Theta)\Gamma(\Theta)}\int_0^{\varkappa}(\varkappa-r)^{\Theta-1}\Psi_1(r,\mathbf{S}_{n-1}(r))\,dr,\\ \mathbf{E}_n(\varkappa)+\mathbf{E}(0)+\dfrac{(1-\Theta)\mathscr{K}^{1-\Theta}}{\aleph(\Theta)}\Psi_2(\varkappa,\mathbf{E}_{n-1}(\varkappa))+\dfrac{\Theta\mathscr{K}^{1-\Theta}}{\aleph(\Theta)\Gamma(\Theta)}\int_0^{\varkappa}(\varkappa-r)^{\Theta-1}\Psi_2(r,\mathbf{E}_{n-1}(r))\,dr,\\ \mathbf{I}_n(\varkappa)=\mathbf{I}(0)+\dfrac{(1-\Theta)\mathscr{K}^{1-\Theta}}{\aleph(\Theta)}\Psi_3(\varkappa,\mathbf{I}_{n-1}(\varkappa))+\dfrac{\Theta\mathscr{K}^{1-\Theta}}{\aleph(\Theta)\Gamma(\Theta)}\int_0^{\varkappa}(\varkappa-r)^{\Theta-1}\Psi_3(r,\mathbf{I}_{n-1}(r))\,dr,\\ \mathbf{V}_n(\varkappa)=\mathbf{V}(0)+\dfrac{(1-\Theta)\mathscr{K}^{1-\Theta}}{\aleph(\Theta)}\Psi_4(\varkappa,\mathbf{V}_{n-1}(\varkappa))+\dfrac{\Theta\mathscr{K}^{1-\Theta}}{\aleph(\Theta)\Gamma(\Theta)}\int_0^{\varkappa}(\varkappa-r)^{\Theta-1}\Psi_4(r,\mathbf{V}_{n-1}(r))\,dr,\\ \mathbf{R}_n(\varkappa)=\mathbf{R}(0)+\dfrac{(1-\Theta)\mathscr{K}^{1-\Theta}}{\aleph(\Theta)}\Psi_5(\varkappa,\mathbf{R}_{n-1}(\varkappa))+\dfrac{\Theta\mathscr{K}^{1-\Theta}}{\aleph(\Theta)\Gamma(\Theta)}\int_0^{\varkappa}(\varkappa-r)^{\Theta-1}\Psi_5(r,\mathbf{R}_{n-1}(r))\,dr. \end{cases} \tag{16}$$

Now, we denote the difference between successive components by Φ_n^i, $i=1,2,\ldots,5$. Therefore,

$$\begin{aligned}\Phi_n^1(\varkappa)=\mathbf{S}_n(\varkappa)-\mathbf{S}_{n-1}(\varkappa) &= \frac{(1-\Theta)\mathscr{K}^{1-\Theta}}{\aleph(\Theta)}\left[\Psi_1(\varkappa,\mathbf{S}_{n-1}(\varkappa))-\Psi_1(\varkappa,\mathbf{S}_{n-2}(\varkappa))\right]\\ &\quad+\frac{\Theta\mathscr{K}^{1-\Theta}}{\aleph(\Theta)\Gamma(\Theta)}\int_0^{\varkappa}(\varkappa-r)^{\Theta-1}\left[\Psi_1(r,\mathbf{S}_{n-1}(r))-\Psi_1(r,\mathbf{S}_{n-2}(r))\right]dr,\\ \Phi_n^2(\varkappa)=\mathbf{E}_n(\varkappa)-\mathbf{E}_{n-1}(\varkappa) &= \frac{(1-\Theta)\mathscr{K}^{1-\Theta}}{\aleph(\Theta)}\left[\Psi_2(\varkappa,\mathbf{E}_{n-1}(\varkappa))-\Psi_2(\varkappa,\mathbf{E}_{n-2}(\varkappa))\right] \end{aligned}$$

$$+\frac{\Theta\mathscr{K}^{1-\Theta}}{\aleph(\Theta)\Gamma(\Theta)}\int_0^{\varkappa}(\varkappa-r)^{\Theta-1}\left[\Psi_2\left(r,\mathbf{E}_{n-1}\left(r\right)\right)-\Psi_2\left(r,\mathbf{E}_{n-2}\left(r\right)\right)\right]dr,$$

$$\Phi_n^3\left(\varkappa\right)=\mathbf{I}_n\left(\varkappa\right)-\mathbf{I}_{n-1}\left(\varkappa\right)=\frac{(1-\Theta)\mathscr{K}^{1-\Theta}}{\aleph(\Theta)}\left[\Psi_3\left(\varkappa,\mathbf{I}_{n-1}\left(\varkappa\right)\right)-\Psi_3\left(\varkappa,\mathbf{I}_{n-2}\left(\varkappa\right)\right)\right]$$
$$+\frac{\Theta\mathscr{K}^{1-\Theta}}{\aleph(\Theta)\Gamma(\Theta)}\int_0^{\varkappa}(\varkappa-r)^{\Theta-1}\left[\Psi_3\left(r,\mathbf{I}_{n-1}\left(r\right)\right)-\Psi_3\left(r,\mathbf{I}_{n-2}\left(r\right)\right)\right]dr,$$

$$\Phi_n^4\left(\varkappa\right)=\mathbf{V}_n\left(\varkappa\right)-\mathbf{V}_{n-1}\left(\varkappa\right)=\frac{(1-\Theta)\mathscr{K}^{1-\Theta}}{\aleph(\Theta)}\left[\Psi_4\left(\varkappa,\mathbf{V}_{n-1}\left(\varkappa\right)\right)-\Psi_4\left(\varkappa,\mathbf{V}_{n-2}\left(\varkappa\right)\right)\right]$$
$$+\frac{\Theta\mathscr{K}^{1-\Theta}}{\aleph(\Theta)\Gamma(\Theta)}\int_0^{\varkappa}(\varkappa-r)^{\Theta-1}\left[\Psi_4\left(r,\mathbf{V}_{n-1}\left(r\right)\right)-\Psi_4\left(r,\mathbf{V}_{n-2}\left(r\right)\right)\right]dr,$$

$$\Phi_n^5\left(\varkappa\right)=\mathbf{R}_n\left(\varkappa\right)-\mathbf{R}_{n-1}\left(\varkappa\right)=\frac{(1-\Theta)\mathscr{K}^{1-\Theta}}{\aleph(\Theta)}\left[\Psi_5\left(\varkappa,\mathbf{R}_{n-1}\left(\varkappa\right)\right)-\Psi_5\left(\varkappa,\mathbf{R}_{n-2}\left(\varkappa\right)\right)\right]$$
$$+\frac{\Theta\mathscr{K}^{1-\Theta}}{\aleph(\Theta)\Gamma(\Theta)}\int_0^{\varkappa}(\varkappa-r)^{\Theta-1}\left[\Psi_5\left(r,\mathbf{R}_{n-1}\left(r\right)\right)-\Psi_5\left(r,\mathbf{R}_{n-2}\left(r\right)\right)\right]dr, \tag{17}$$

Taking into account that

$$\begin{cases}\mathbf{S}_n\left(\varkappa\right)=\sum_{i=0}^{n}\Phi_i^1\left(\varkappa\right),\mathbf{E}_n\left(\varkappa\right)=\sum_{i=0}^{n}\Phi_i^2\left(\varkappa\right),\mathbf{I}_n\left(\varkappa\right)=\sum_{i=0}^{n}\Phi_i^3\left(\varkappa\right),\\ \mathbf{V}_n\left(\varkappa\right)=\sum_{i=0}^{n}\Phi_i^4\left(\varkappa\right),\mathbf{R}_n\left(\varkappa\right)=\sum_{i=0}^{n}\Phi_i^5\left(\varkappa\right).\end{cases} \tag{18}$$

Then, we take the norm on both sides of Eq. (17). It follows from Eqs. (14) and (15) that

$$\left\|\Phi_n^1(\varkappa)\right\|=\frac{(1-\Theta)\mathscr{K}^{1-\Theta}L_1}{\aleph(\Theta)}\left\|\Phi_{n-1}^1\left(\varkappa\right)\right\|+\frac{\Theta\mathscr{K}^{1-\Theta}L_1}{\aleph(\Theta)\Gamma(\Theta)}\int_0^{\varkappa}(\varkappa-r)^{\Theta-1}\left\|\Phi_{n-1}^1\left(r\right)\right\|dr,$$
$$\left\|\Phi_n^2(\varkappa)\right\|=\frac{(1-\Theta)\mathscr{K}^{1-\Theta}L_2}{\aleph(\Theta)}\left\|\Phi_{n-1}^2\left(\varkappa\right)\right\|+\frac{\Theta\mathscr{K}^{1-\Theta}L_2}{\aleph(\Theta)\Gamma(\Theta)}\int_0^{\varkappa}(\varkappa-r)^{\Theta-1}\left\|\Phi_{n-1}^2\left(r\right)\right\|dr,$$
$$\left\|\Phi_n^3(\varkappa)\right\|=\frac{(1-\Theta)\mathscr{K}^{1-\Theta}L_3}{\aleph(\Theta)}\left\|\Phi_{n-1}^3\left(\varkappa\right)\right\|+\frac{\Theta\mathscr{K}^{1-\Theta}L_3}{\aleph(\Theta)\Gamma(\Theta)}\int_0^{\varkappa}(\varkappa-r)^{\Theta-1}\left\|\Phi_{n-1}^3\left(r\right)\right\|dr,$$
$$\left\|\Phi_n^4(\varkappa)\right\|=\frac{(1-\Theta)\mathscr{K}^{1-\Theta}L_4}{\aleph(\Theta)}\left\|\Phi_{n-1}^4\left(\varkappa\right)\right\|+\frac{\Theta\mathscr{K}^{1-\Theta}L_4}{\aleph(\Theta)\Gamma(\Theta)}\int_0^{\varkappa}(\varkappa-r)^{\Theta-1}\left\|\Phi_{n-1}^4\left(r\right)\right\|dr,$$
$$\left\|\Phi_n^5(\varkappa)\right\|=\frac{(1-\Theta)\mathscr{K}^{1-\Theta}L_5}{\aleph(\Theta)}\left\|\Phi_{n-1}^5\left(\varkappa\right)\right\|+\frac{\Theta\mathscr{K}^{1-\Theta}L_5}{\aleph(\Theta)\Gamma(\Theta)}\int_0^{\varkappa}(\varkappa-r)^{\Theta-1}\left\|\Phi_{n-1}^5\left(r\right)\right\|dr. \tag{19}$$

Next, we shall prove the main theorem based on the above results.

Theorem 5.2. The fractional models (3)–(4) has a unique solution for $\varkappa\in[0,\,T]$ if

$$\left(\frac{(1-\Theta)\mathscr{K}^{1-\Theta}}{\aleph(\Theta)}+\frac{\mathscr{K}^{1-\Theta}T^{\Theta}}{\aleph(\Theta)\Gamma(\Theta)}\right)L_1<1. \tag{20}$$

Proof. Since S(t), E(t), I(t), V(t), and R(t) are bounded functions and satisfying the Lipschitz condition. Therefore, by virtue of Eq. (19), we obtain

$$\begin{aligned}
\left|\left|\Phi_n^1(\varkappa)\right|\right| &\leq ||\mathbf{S}_n(0)||\left[\frac{(1-\Theta)\mathscr{K}^{1-\Theta}L_1}{\aleph(\Theta)}+\frac{T^{\Theta}\mathscr{K}^{1-\Theta}L_1}{\aleph(\Theta)\Gamma(\Theta)}\right]^n,\\
\left|\left|\Phi_n^2(\varkappa)\right|\right| &\leq ||\mathbf{E}_n(0)||\left[\frac{(1-\Theta)\mathscr{K}^{1-\Theta}L_2}{\aleph(\Theta)}+\frac{T^{\Theta}\mathscr{K}^{1-\Theta}L_2}{\aleph(\Theta)\Gamma(\Theta)}\right]^n,\\
\left|\left|\Phi_n^3(\varkappa)\right|\right| &\leq ||\mathbf{I}_n(0)||\left[\frac{(1-\Theta)\mathscr{K}^{1-\Theta}L_3}{\aleph(\Theta)}+\frac{T^{\Theta}\mathscr{K}^{1-\Theta}L_3}{\aleph(\Theta)\Gamma(\Theta)}\right]^n,\\
\left|\left|\Phi_n^4(\varkappa)\right|\right| &\leq ||\mathbf{V}_n(0)||\left[\frac{(1-\Theta)\mathscr{K}^{1-\Theta}L_4}{\aleph(\Theta)}+\frac{T^{\Theta}\mathscr{K}^{1-\Theta}L_4}{\aleph(\Theta)\Gamma(\Theta)}\right]^n,\\
\left|\left|\Phi_n^5(\varkappa)\right|\right| &\leq ||\mathbf{R}_n(0)||\left[\frac{(1-\Theta)\mathscr{K}^{1-\Theta}L_5}{\aleph(\Theta)}+\frac{T^{\Theta}\mathscr{K}^{1-\Theta}L_5}{\aleph(\Theta)\Gamma(\Theta)}\right]^n.
\end{aligned} \tag{21}$$

Consequently, the sequences in Eq. (21) are exist and smooth, i.e., $\left|\left|\Phi_n^i(\varkappa)\right|\right| \to 0$, $(i=1,2,\ldots,5)$ as $n \to \infty$.

Now, we show that the functions in Eq. (21) are the solutions of the proposed model. We suppose

$$\begin{aligned}
\mathbf{S}(\varkappa)-\mathbf{S}(0) &= \mathbf{S}_n(\varkappa)-F_n^1(\varkappa),\\
\mathbf{E}(\varkappa)-\mathbf{E}(0) &= \mathbf{E}_n(\varkappa)-F_n^2(\varkappa),\\
\mathbf{I}(\varkappa)-\mathbf{I}(0) &= \mathbf{I}_n(\varkappa)-F_n^3(\varkappa),\\
\mathbf{V}(\varkappa)-\mathbf{V}(0) &= \mathbf{V}_n(\varkappa)-F_n^4(\varkappa),\\
\mathbf{R}(\varkappa)-\mathbf{R}(0) &= \mathbf{R}_n(\varkappa)-F_n^5(\varkappa).
\end{aligned} \tag{22}$$

Then we show that the terms in Eq. (22) verify that $\left|\left|F_n^i(\varkappa)\right|\right| \to 0$, as $n \to \infty$, $(i=1,2,\ldots,5)$. Thus, we have

$$\begin{aligned}
||F_n^1(\varkappa)|| &= \left|\left|\frac{(1-\Theta)\mathscr{K}^{1-\Theta}}{\aleph(\Theta)}\left[\Psi_1(\varkappa,\mathbf{S}(\varkappa))-\Psi_1(\varkappa,\mathbf{S}_{n-1}(\varkappa)\right]\right.\right.\\
&\quad\left.\left.+\frac{\Theta\mathscr{K}^{1-\Theta}}{\aleph(\Theta)\Gamma(\Theta)}\int_0^{\varkappa}(\varkappa-r)^{\Theta-1}\left[\Psi_1(r,\mathbf{S}(r))-\Psi_1(r,\mathbf{S}_{n-1}(r))\right]dr\right|\right|\\
&\leq \frac{(1-\Theta)\mathscr{K}^{1-\Theta}}{\aleph(\Theta)}||\Psi_1(\varkappa,\mathbf{S}(\varkappa))-\Psi_1(\varkappa,\mathbf{S}_{n-1}(\varkappa)||\\
&\quad+\frac{\Theta\mathscr{K}^{1-\Theta}}{\aleph(\Theta)\Gamma(\Theta)}\int_0^{\varkappa}(\varkappa-r)^{\Theta-1}||\Psi_1(r,\mathbf{S}(r))-\Psi_1(r,\mathbf{S}_{n-1}(r))||dr\\
&\leq \left(\frac{(1-\Theta)\mathscr{K}^{1-\Theta}}{\aleph(\Theta)}+\frac{\mathscr{K}^{1-\Theta}T^{\Theta}}{\aleph(\Theta)\Gamma(\Theta)}\right)L_1||\mathbf{S}(\varkappa)-\mathbf{S}_{n-1}(\varkappa)||.
\end{aligned}$$

Repeating the procedure above, we get

$$\left|\left|F_n^1(\varkappa)\right|\right| \leq \left(\frac{(1-\Theta)\mathscr{K}^{1-\Theta}}{\aleph(\Theta)}+\frac{\mathscr{K}^{1-\Theta}T^{\Theta}}{\aleph(\Theta)\Gamma(\Theta)}\right)^{n+1}L_1^{n+1}M.$$

As $n \to \infty$, $\left|\left|F_n^1(\varkappa)\right|\right| \to 0$.By the same arguments above, it can be shown that $\left|\left|F_n^i(\varkappa)\right|\right| \to 0$, as $n \to \infty$, $(i = 2, 3, \ldots, 5)$.

To prove the uniqueness result, we assume that the model (3) has another solution $(\mathbf{S}^\star(\varkappa), \mathbf{E}^\star(\varkappa), \mathbf{I}^\star(\varkappa), \mathbf{V}^\star(\varkappa), \mathbf{R}^\star(\varkappa))$. Then

$$\begin{aligned}||\mathbf{S}(\varkappa) - \mathbf{S}^\star(\varkappa)|| &\leq \frac{(1-\Theta)\mathscr{K}^{1-\Theta}}{\aleph(\Theta)}||\Psi_1(\varkappa, \mathbf{S}(\varkappa)) - \Psi_1(\varkappa, \mathbf{S}^\star(\varkappa)||\\ &+ \frac{\Theta\mathscr{K}^{1-\Theta}}{\aleph(\Theta)\Gamma(\Theta)}\int_0^\varkappa (\varkappa - r)^{\Theta-1}||\Psi_1(r, \mathbf{S}(r)) - \Psi_1(r, \mathbf{S}^\star(r))||dr\\ &\leq \left(\frac{(1-\Theta)\mathscr{K}^{1-\Theta}}{\aleph(\Theta)} + \frac{\mathscr{K}^{1-\Theta}T^\Theta}{\aleph(\Theta)\Gamma(\Theta)}\right)L_1||\mathbf{S}(\varkappa) - \mathbf{S}^\star(\varkappa)||,\end{aligned}$$

which implies

$$\left[1 - \left(\frac{(1-\Theta)\mathscr{K}^{1-\Theta}}{\aleph(\Theta)} + \frac{\mathscr{K}^{1-\Theta}T^\Theta}{\aleph(\Theta)\Gamma(\Theta)}\right)L_1\right]\left|\left|\mathbf{S}(\varkappa) - \mathbf{S}^\star(\varkappa)\right|\right| \leq 0.$$

It is clear that $\mathbf{S}(\varkappa) = \mathbf{S}^\star(\varkappa)$, if the following inequality is satisfied

$$\left[1 - \left(\frac{(1-\Theta)\mathscr{K}^{1-\Theta}}{\aleph(\Theta)} + \frac{\mathscr{K}^{1-\Theta}T^\Theta}{\aleph(\Theta)\Gamma(\Theta)}\right)L_1\right] > 0.$$

This is satisfied by the hypothesis (20). Hence, $\mathbf{S}(\varkappa) = \mathbf{S}^\star(\varkappa)$.

Similarly, we obtain $\mathbf{E}(\varkappa) = \mathbf{E}^\star(\varkappa)$, $\mathbf{I}(\varkappa) = \mathbf{I}^\star(\varkappa)$, $\mathbf{V}(\varkappa) = \mathbf{V}^\star(\varkappa)$, and $\mathbf{R}(\varkappa) = \mathbf{R}^\star(\varkappa)$.

6 Numerical Results

This section gives the numerical solution of the COVID-19 model (3) under ABC fractional derivatives. The suggested fractional model is addressed numerically using a generalized Adams–Bashforth–Moulton technique [44,45].

By applying the operator ${}^{AB}\Im^\Theta$ on the first equation of (11), we obtain

$$\mathbf{S}(\varkappa) - \mathbf{S}(0) = \frac{(1-\Theta)\mathscr{K}^{1-\Theta}}{\aleph(\Theta)}\Psi_1(\varkappa, \mathbf{S}) + \frac{\Theta\mathscr{K}^{1-\Theta}}{\aleph(\Theta)\Gamma(\Theta)}\int_0^\varkappa (\varkappa - r)^{\Theta-1}\Psi_1(r, \mathbf{S})\, dr.$$

For $\varkappa = \varkappa_{n+1}$, $n = 0, 1, 2, \ldots$, we get

$$\begin{aligned}\mathbf{S}(\varkappa_{n+1}) &= \mathbf{S}_0 + \frac{(1-\Theta)\mathscr{K}^{1-\Theta}}{\aleph(\Theta)}\Psi_1(\varkappa_n, \mathbf{S}) + \frac{\Theta\mathscr{K}^{1-\Theta}}{\aleph(\Theta)\Gamma(\Theta)}\int_0^{\varkappa_{n+1}} (\varkappa_{n+1} - r)^{\Theta-1}\Psi_1(r, \mathbf{S})\, dr\\ &= \mathbf{S}_0 + \frac{(1-\Theta)\mathscr{K}^{1-\Theta}}{\aleph(\Theta)}\Psi_1(\varkappa_n, \mathbf{S}) + \frac{\Theta\mathscr{K}^{1-\Theta}}{\aleph(\Theta)\Gamma(\Theta)}\sum_{s=0}^{n}\int_{\varkappa_s}^{\varkappa_{s+1}} (\varkappa_{n+1} - r)^{\Theta-1}\Psi_1(r, \mathbf{S})\, dr.\end{aligned}$$

Over $[\varkappa_s, \varkappa_{s+1}]$, the function $\Psi_1(r, \mathbf{S})$ can be approximated by the interpolation polynomial

$$\begin{aligned}P(s, r) &= \frac{r - \varkappa_{s-1}}{\varkappa_s - \varkappa_{s-1}}\mathbf{G}(\varkappa_s, \mathbf{Z}(\varkappa_s)) - \frac{r - \varkappa_s}{\varkappa_s - \varkappa_{s-1}}\mathbf{G}(\varkappa_{s-1}, \mathbf{Z}(\varkappa_{s-1}))\\ &= \frac{\mathbf{G}(\varkappa_s, \mathbf{Z}(\varkappa_s))}{h}(r - \varkappa_{s-1}) - \frac{\mathbf{G}(\varkappa_{s-1}, \mathbf{Z}(\varkappa_{s-1}))}{h}(r - \varkappa_s)\\ &\approx \frac{\mathbf{G}(\varkappa_s, \mathbf{Z}_s)}{h}(r - \varkappa_{s-1}) - \frac{\mathbf{G}(\varkappa_{s-1}, \mathbf{Z}_{s-1})}{h}(r - \varkappa_s),\end{aligned}$$

which implies

$$\mathbf{S}\left(\varkappa_{n+1}\right)=\mathbf{S}_0+\frac{(1-\Theta)\mathscr{K}^{1-\Theta}}{\aleph(\Theta)}\Psi_1\left(\varkappa_n,\mathbf{S}\right)$$
$$+\frac{\Theta\mathscr{K}^{1-\Theta}}{\aleph(\Theta)\Gamma(\Theta)}\sum_{s=0}^{n}\left\{\frac{\Psi_1(\varkappa_s,\mathbf{S})}{h}\int_{\varkappa_s}^{\varkappa_{s+1}}\left(\varkappa_{n+1}-r\right)^{\Theta-1}\left(r-\varkappa_{s-1}\right)dr\right.$$
$$\left.-\frac{\Psi_1(\varkappa_{s-1},\mathbf{S})}{h}\int_{\varkappa_s}^{\varkappa_{s+1}}\left(\varkappa_{n+1}-r\right)^{\Theta-1}\left(r-\varkappa_s\right)dr.\right.$$

Set $\mathbb{I}_{\Theta,1}:=\int_{\varkappa_s}^{\varkappa_{s+1}}(\varkappa_{n+1}-r)^{\Theta-1}(r-\varkappa_{s-1})dr$ and $\mathbb{I}_{\Theta,2}:=\int_{\varkappa_s}^{\varkappa_{s+1}}(\varkappa_{n+1}-r)^{\Theta-1}(r-\varkappa_s)dr$. Evaluating these integrals, we obtain

$$\mathbb{I}_{\Theta,1}=h^{\Theta+1}\frac{(n+1-s)^{\Theta}(n-s+\Theta+2)-(n-s)^{\Theta}(n-s+2\Theta+2)}{\Theta(\Theta+1)},$$

$$\mathbb{I}_{\Theta,2}=h^{\Theta+1}\frac{(n+1-s)^{\Theta}-(n-s)^{\Theta}(n-s+\Theta+1)}{\Theta(\Theta+1)}.$$

Finally,

$$\mathbf{S}\left(\varkappa_{n+1}\right)=\mathbf{S}_0+\frac{(1-\Theta)\mathscr{K}^{1-\Theta}}{\aleph(\Theta)}\Psi_1\left(\varkappa_n,\mathbf{S}\right)+\frac{\Theta\mathscr{K}^{1-\Theta}}{\aleph(\Theta)\Gamma(\Theta)}\sum_{s=0}^{n}$$
$$\left\{h^{\Theta}\frac{\Psi_1(\varkappa_s,\mathbf{S})}{\Gamma(\Theta+2)}\left[\left(n+1-s\right)^{\Theta}\left(n-s+\Theta+2\right)-\left(n-s\right)^{\Theta}\left(n-s+2\Theta+2\right)\right]\right.$$
$$\left.-h^{\Theta}\frac{\Psi_1(\varkappa_{s-1},\mathbf{S})}{\Gamma(\Theta+2)}\left[\left(n+1-s\right)^{\Theta}-\left(n-s\right)^{\Theta}\left(n-s+\Theta+1\right)\right].\right. \tag{23}$$

In an analogous manner for the remainder of the equations of the model (3), we obtain the recursive formulae as below:

$$\mathbf{E}\left(\varkappa_{n+1}\right)=\mathbf{E}_0+\frac{(1-\Theta)\mathscr{K}^{1-\Theta}}{\aleph(\Theta)}\Psi_1\left(\varkappa_n,\mathbf{E}\right)+\frac{\Theta\mathscr{K}^{1-\Theta}}{\aleph(\Theta)\Gamma(\Theta)}\sum_{s=0}^{n}$$
$$\left\{h^{\Theta}\frac{\Psi_1(\varkappa_s,\mathbf{E})}{\Gamma(\Theta+2)}\left[\left(n+1-s\right)^{\Theta}\left(n-s+\Theta+2\right)-\left(n-s\right)^{\Theta}\left(n-s+2\Theta+2\right)\right]\right.$$
$$\left.-h^{\Theta}\frac{\Psi_1(\varkappa_{s-1},\mathbf{E})}{\Gamma(\Theta+2)}\left[\left(n+1-s\right)^{\Theta}-\left(n-s\right)^{\Theta}\left(n-s+\Theta+1\right)\right].\right. \tag{24}$$

$$\mathbf{I}\left(\varkappa_{n+1}\right)=\mathbf{I}_0+\frac{(1-\Theta)\mathscr{K}^{1-\Theta}}{\aleph(\Theta)}\Psi_1\left(\varkappa_n,\mathbf{I}\right)+\frac{\Theta\mathscr{K}^{1-\Theta}}{\aleph(\Theta)\Gamma(\Theta)}\sum_{s=0}^{n}$$
$$\left\{h^{\Theta}\frac{\Psi_1(\varkappa_s,\mathbf{I})}{\Gamma(\Theta+2)}\left[\left(n+1-s\right)^{\Theta}\left(n-s+\Theta+2\right)-\left(n-s\right)^{\Theta}\left(n-s+2\Theta+2\right)\right]\right.$$
$$\left.-h^{\Theta}\frac{\Psi_1(\varkappa_{s-1},\mathbf{I})}{\Gamma(\Theta+2)}\left[\left(n+1-s\right)^{\Theta}-\left(n-s\right)^{\Theta}\left(n-s+\Theta+1\right)\right].\right. \tag{25}$$

$$\mathbf{V}\left(\varkappa_{n+1}\right)=\mathbf{V}_0+\frac{(1-\Theta)\mathscr{K}^{1-\Theta}}{\aleph(\Theta)}\Psi_1\left(\varkappa_n,\mathbf{V}\right)+\frac{\Theta\mathscr{K}^{1-\Theta}}{\aleph(\Theta)\Gamma(\Theta)}\sum_{s=0}^{n}$$
$$\left\{h^{\Theta}\frac{\Psi_1(\varkappa_s,\mathbf{V})}{\Gamma(\Theta+2)}\left[(n+1-s)^{\Theta}(n-s+\Theta+2)-(n-s)^{\Theta}(n-s+2\Theta+2)\right]\right.$$
$$\left.-h^{\Theta}\frac{\Psi_1(\varkappa_{s-1},\mathbf{V})}{\Gamma(\Theta+2)}\left[(n+1-s)^{\Theta}-(n-s)^{\Theta}(n-s+\Theta+1)\right]\right. \tag{26}$$

$$\mathbf{R}\left(\varkappa_{n+1}\right)=\mathbf{R}_0+\frac{(1-\Theta)\mathscr{K}^{1-\Theta}}{\aleph(\Theta)}\Psi_1\left(\varkappa_n,\mathbf{R}\right)+\frac{\Theta\mathscr{K}^{1-\Theta}}{\aleph(\Theta)\Gamma(\Theta)}\sum_{s=0}^{n}$$
$$\left\{h^{\Theta}\frac{\Psi_1(\varkappa_s,\mathbf{R})}{\Gamma(\Theta+2)}\left[(n+1-s)^{\Theta}(n-s+\Theta+2)-(n-s)^{\Theta}(n-s+2\Theta+2)\right]\right.$$
$$\left.-h^{\Theta}\frac{\Psi_1(\varkappa_{s-1},\mathbf{R})}{\Gamma(\Theta+2)}\left[(n+1-s)^{\Theta}-(n-s)^{\Theta}(n-s+\Theta+1)\right]\right. \tag{27}$$

7 Simulations Results

The biological parameters estimated from the actual data reported in KSA for the period June 01, 2021 to February 15, 2022, and classified in Table 7 is used to acquire the simulation results. Further for initial data we use S(0) = 9.317558 millions, E(0) = 0, I(0) = 0.562300 million, V(0) = 24.000000 millions, R(0) = 0.580000 million, where N = 34.810000 millions is a total population. For the purposes of numerical simulations, the high estimate of 24,000,000 vaccinated population is considered to account for any uncertainty in the estimate for the current total number of vaccinated individuals population in KSA. We simulate the results for the given 300 days as in Figs. 6–10.

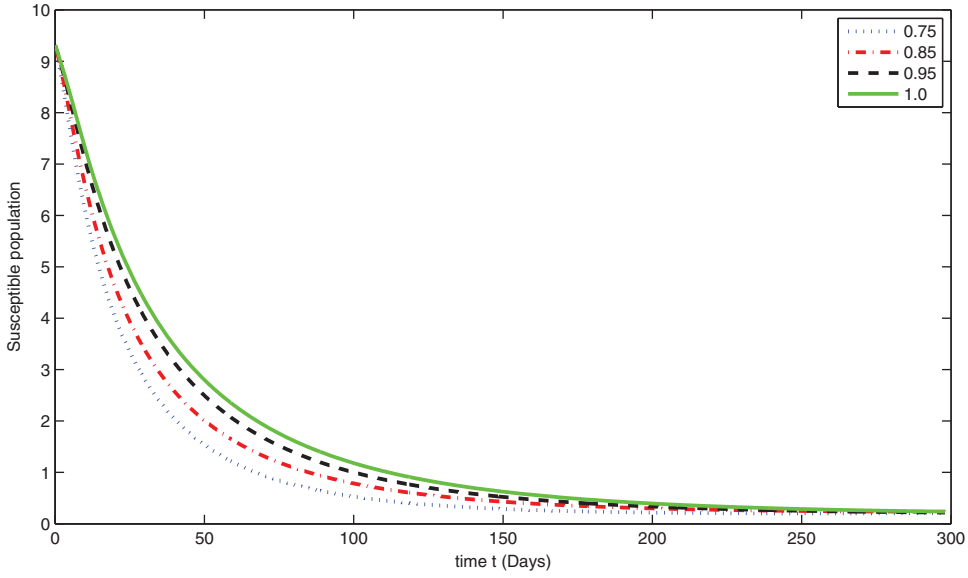

Figure 6: Graphical presentation for different fractional order of the susceptible class for the considered model

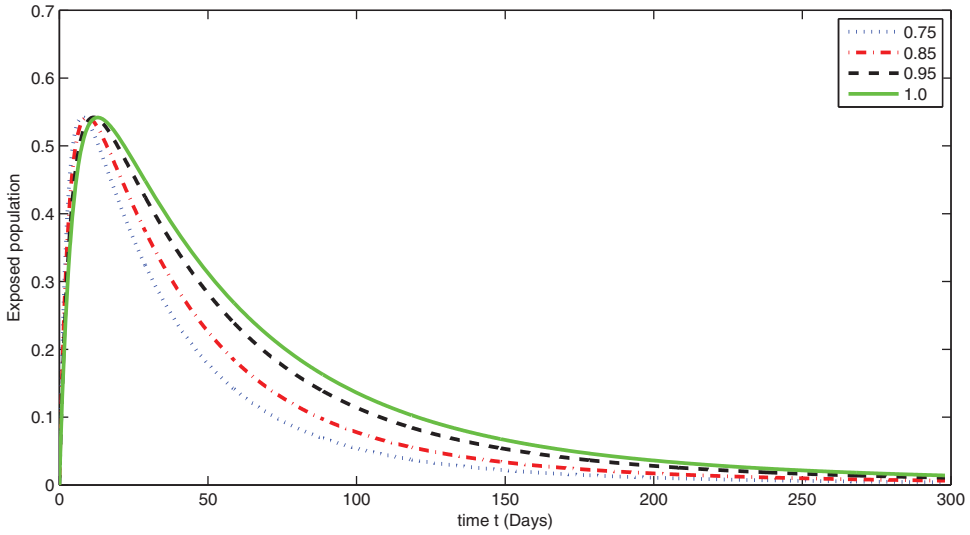

Figure 7: Graphical presentation for different fractional order of the exposed class for the considered model

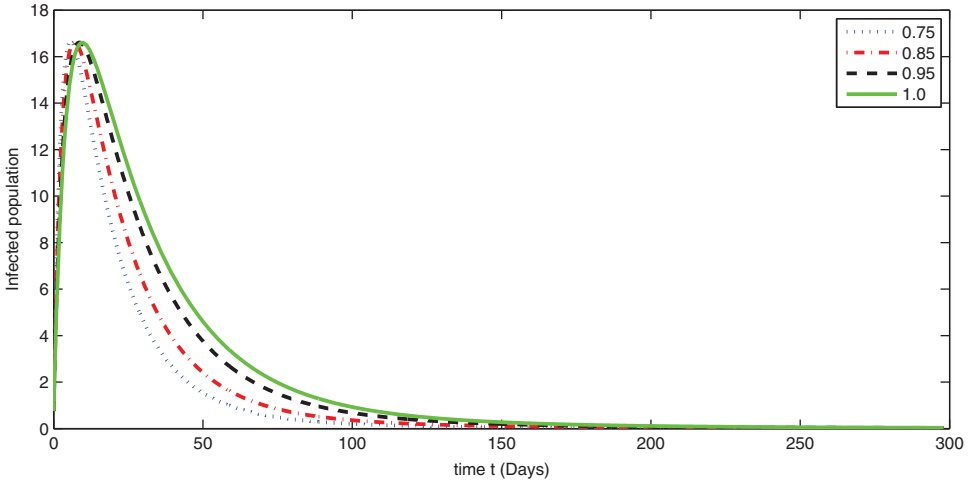

Figure 8: Graphical presentation for different fractional order of the infected class for the considered model

We see that corresponding to different fractional order, the susceptible class is decreasing with various scenario in Fig. 6. Consequently the density of exposed class is also behave like susceptible at various fractional order, see Fig. 7. The infected class first increase then starts to decline (see Fig. 8) due to vaccination process until become stable as in Fig. 9. Thanking to vaccination the decline in infection will cause the increase in recovery class whose dynamics shows variation due to different fractional order as in Fig. 10. From these graphical presentations we observe the transmission dynamics in the presence of vaccine by using fractional order derivative. The fractional calculus helps us in better understanding of the transmission dynamics in a locality. Also the impact of vaccine is importance which understand from the recovery class presentation. Next, we compared the simulated plots of the

population have been fully vaccinated in Fig. 11 with the graphs at different fractional order. We see that graphs are closely agreed which demonstrates the efficiency of our proposed model.

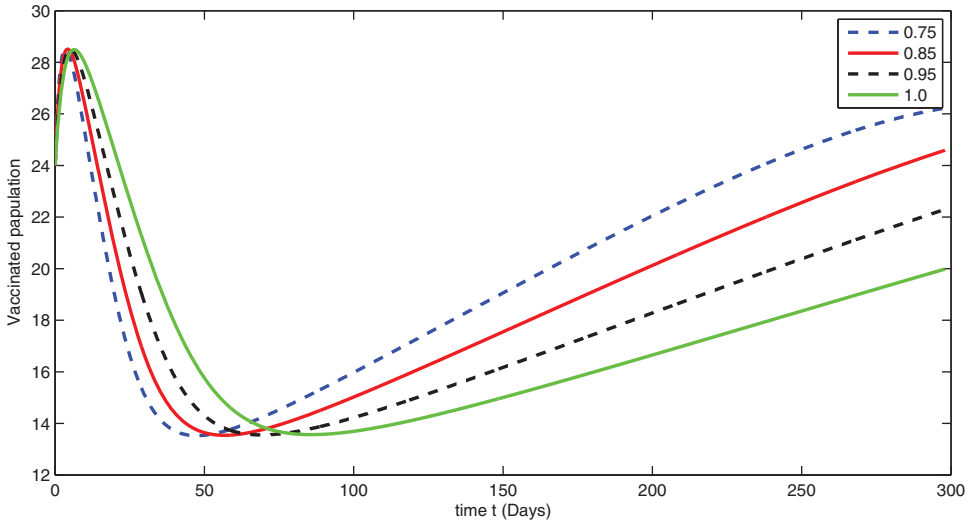

Figure 9: Graphical presentation for different fractional order of the vaccinated class for the considered model

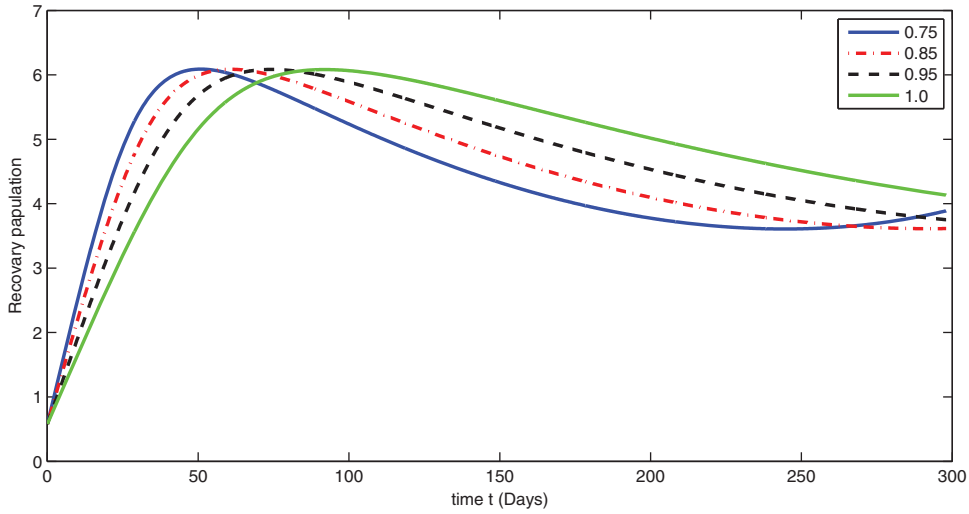

Figure 10: Graphical presentation for different fractional order of the recovered class for the considered model

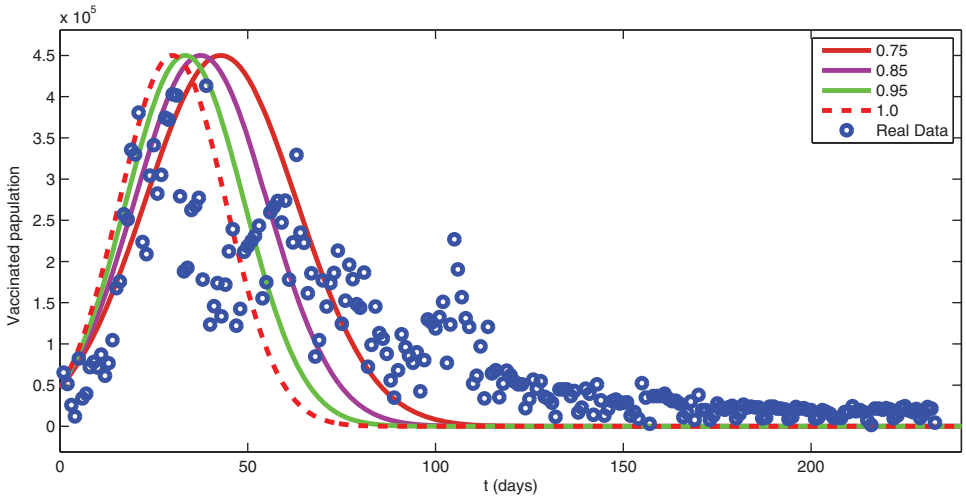

Figure 11: Comparison of real data with different fractional order simulation

8 Conclusion

In this research work, we have updated a COVID-19 model to a fractional order derivative of generalized type. On the statistical aspect, we have used some statistical analysis to collect data on vaccination in KSA for 300 days, and then the concerned statistical analysis has been shown. Consequently, the forecast about the evolution of the COVID-19 vaccination in 60 days has been presented. We have found, through the ARIMA(1, 1, 2) model, a decrease in the number of people who have been given full doses with (927164), and they constitute 2.6% of the total population in KSA. Data analysis showed that 67.81% of the population had been fully vaccinated during the study period. On the analytical aspect, we have established some adequate results for the existence and uniqueness of the solution through fixed point techniques. The respective results are important because a mathematical formulation should be preferentially checked for their existence. Finally, in terms of numerical aspects, we have extended the Adam-Bashforth method for the considered model to derive a scheme for numerical analysis. Moreover, we have then used the real data for parameters and some initial data of KSA to see the transmission dynamics of COVID-19 with the vaccinated class. Finally, the concerned numerical simulations have been compared with the exact real available date given in Section 2. We see that the real data plot and simulated data plots coincide very well. This phenomenon demonstrates the applicability of the method.

Authors' Contributions: All authors contributed equally and significantly in writing this paper. All authors read and approved the final manuscript.

Acknowledgement: The authors would like to thank Imam Mohammad Ibn Saud Islamic University (IMSIU), for funding this research work.

Data Availability Statement: Data are available upon request.

Funding Statement: This research was supported by the Deanship of Scientific Research, Imam Mohammad Ibn Saud Islamic University (IMSIU), Saudi Arabia, Grant No. (21-13-18-069).

Conflicts of Interest: The authors declare that they have no conflicts of interest to report regarding the present study.

References

1. Hu, B., Guo, H., Zhou, P., Shi, Z. L. (2021). Characteristics of SARS-CoV-2 and COVID-19. *Nature Reviews Microbiology, 19,* 141–154. DOI 10.1038/s41579-020-00459-7.
2. WHO (2021). World Health Organization Weakly Report. https://www.who.int/emergencies/diseases/novel-coronavirus-2019.
3. Worldometers.info (2021). Coronavirus cases-worldometer. https://www.worldometers.info/coronavirus.
4. FDA, U.S. FOOD & DRUG. COVID-19 Vaccines (2022). https://www.fda.gov/emergency-preparedness-and-response/coronavirus-disease-2019-covid-19/covid-19-vaccines.
5. Mathevet, T., Lepiller, M., Mangin, A. (2004). Application of time series analyses to the hydrological functioning of an alpine karstic system: The case of Bange-L'Eua-Morte. *Hydrology and Earth System Sciences, 8(6),* 1051–1064. DOI 10.5194/hess-8-1051-2004.
6. Khan, F., Pilz, J. (2018). Modelling and sensitivity analysis of river flow in the upper Indus basin: Pakistan. *International Journal of Water, 12(1),* 1–21. DOI 10.1504/IJW.2018.090184.
7. Box, G., Jenkins, G. (1970). *Time series analysis, forecasting and control*. San Francisco: Holden-Day.
8. Maleki, M., Mahmoudi, M. R., Wraith, D., Pho, K. H. (2020). Time series modelling to forecast the confirmed and recovered cases of COVID-19. *Travel Medicine and Infectious Disease, 37,* 101742. DOI 10.1016/j.tmaid.2020.101742.
9. Podlubny, I. (1999). *Fractional differential equations*. San Diego: Academic Press.
10. Samko, S. G., Kilbas, A. A., Marichev, O. I. (1993). *Fractional integrals and derivatives*. Yverdon: Gordon & Breach.
11. Kilbas, A. A., Srivastava, H. M., Trujillo, J. J. (2006). *Theory and applications of fractional differential equations*. Amsterdam: North-Holland Mathematics Studies, Elsevier.
12. Ross, B. (2006). A brief history and exposition of the fundamental theory of fractional calculus. *Fractional Calculus and Its Applications, 457,* 1–36. DOI 10.1007/BFb0067096.
13. Yang, X. J. (2019). *General fractional derivatives: Theory, methods and applications*. Chapman and Hall/CRC. DOI 10.1201/9780429284083.
14. Toufik, M., Atangana, A. (2017). New numerical approximation of fractional derivative with non-local and non-singular kernel: Application to chaotic models. *The European Physical Journal Plus, 132(10),* 1–16.
15. Koca, I. (2018). Modelling the spread of Ebola virus with Atangana-Baleanu fractional operators. *The European Physical Journal Plus, 133(3),* 100. DOI 10.1140/epjp/i2018-11949-4.
16. Atangana, A., Gomez-Aguilar, J. F. (2018). Decolonisation of fractional calculus rules: Breaking commutativity and associativity to capture more natural phenomena. *The European Physical Journal Plus, 133(4),* 166. DOI 10.1140/epjp/i2018-12021-3.
17. Tateishi, A. A., Ribeiro, H. V., Lenzi, E. K. (2017). The role of fractional time-derivative operators on anomalous diffusion. *Frontiers in Physics, 52(5),* 19. DOI 10.3389/fphy.2017.00052.
18. Caputo, M., Fabrizio, M. (2015). A new definition of fractional derivative without singular kernel. *Progress in Fractional Differentiation and Applications, 1(2),* 73–85.
19. Losada, J., Nieto, J. J. (2015). Properties of a new fractional derivative without singular kernel. *Progress in Fractional Differentiation and Applications, 1(2),* 87–92.
20. Atangana, A., Baleanu, D. (2016). New fractional derivative with non-local and non-singular kernel. *Thermal Science, 20(2),* 757–763. DOI 10.2298/TSCI160111018A.

21. Jarad, F., Abdeljawad, T., Hammouch, Z. (2018). On a class of ordinary differential equations in the frame of Atangana-Baleanu fractional derivative. *Chaos Solitons Fractals, 117,* 16–20. DOI 10.1016/j.chaos.2018.10.006.
22. Abdeljawad, T. (2017). A Lyapunov type inequality for fractional operators with nonsingular Mittag-Leffler kernel. *Journal of Inequalities and Applications, 2017(1),* 130. DOI 10.1186/s13660-017-1400-5.
23. Atangana, A. (2018). Non validity of index law in fractional calculus: A fractional differential operator with Markovian and non-Markovian properties. *Physica A: Statistical Mechanics and Its Applications, 505,* 688–706. DOI 10.1016/j.physa.2018.03.056.
24. Atangana, A., Gomez-Aguilar, J. F. (2018). Fractional derivatives with no-index law property: Application to chaos and statistics. *Chaos Solitons Fractals, 114,* 516–535. DOI 10.1016/j.chaos.2018.07.033.
25. Abdo, M. S., Shah, K., Wahash, H. A., Panchal, S. K. (2020). On a comprehensive model of the novel coronavirus (COVID-19) under Mittag-Leffler derivative. *Chaos Solitons Fractals, 135,* 109867. DOI 10.1016/j.chaos.2020.109867.
26. Almalahi, M. A., Panchal, S. K., Shatanawi, W., Abdo, M. S., Shah, K. et al. (2021). Analytical study of transmission dynamics of 2019-nCoV pandemic via fractal fractional operator. *Results in Physics, 24,* 104045. DOI 10.1016/j.rinp.2021.104045.
27. Jeelani, M. B., Alnahdi, A. S., Abdo, M. S., Abdulwasaa, M. A., Shah, K. et al. (2021). Mathematical modeling and forecasting of COVID-19 in Saudi Arabia under fractal-fractional derivative in caputo sense with power-law. *Axioms, 10(3),* 228. DOI 10.3390/axioms10030228.
28. Abdulwasaa, M. A., Abdo, M. S., Shah, K., Nofal, T. A., Panchal, S. K. et al. (2021). Fractal-fractional mathematical modeling and forecasting of new cases and deaths of COVID-19 epidemic outbreaks in India. *Results in Physics, 20,* 103702. DOI 10.1016/j.rinp.2020.103702.
29. Atangana, A. (2020). Modelling the spread of COVID-19 with new fractal-fractional operators: Can the lockdown save mankind before vaccination. *Chaos Solitons Fractals, 136,* 109860. DOI 10.1016/j.chaos.2020.109860.
30. Zhang, Z. (2020). A novel COVID-19 mathematical model with fractional derivatives: Singular and nonsingular kernels. *Chaos Solitons Fractals, 139,* 110060. DOI 10.1016/j.chaos.2020.110060.
31. Khan, A., Alshehri, H. M., Abdeljawad, T., Al-Mdallal, Q. M., Khan, H. (2021). Stability analysis of fractional nabla difference COVID-19 model. *Results in Physics, 22,* 103888. DOI 10.1016/j.rinp.2021.103888.
32. Khan, Z. A., Khan, A., Abdeljawad, T., Khan, H. (2022). Computational analysis of fractional order imperfect testing infection disease model. *Fractals*. DOI 10.1142/S0218348X22401697.
33. Ullah, I., Ahmad, S., Al-Mdallal, Q., Khan, Z. A., Khan, H. et al. (2020). Stability analysis of a dynamical model of tuberculosis with incomplete treatment. *Advances in Difference Equations, 2020,* 499. DOI 10.1186/s13662-020-02950-0.
34. Shah, K., Khan, Z. A., Ali, A., Amin, R., Khan, H. et al. (2020). Haar wavelet collocation approach for the solution of fractional order COVID-19 model using caputo derivative. *Alexandria Engineering Journal, 59(5),* 3221–3231. DOI 10.1016/j.aej.2020.08.028.
35. Habenom, H., Aychluh, M., Suthar, D. L., Al-Mdallal, Q., Purohit, S. D. (2022). Modeling and analysis on the transmission of COVID-19 pandemic in Ethiopia. *Alexandria Engineering Journal, 61(7),* 5323–5342. DOI 10.1016/j.aej.2021.10.054.
36. Bozkurt, F., Yousef, A., Abdeljawad, T., Kalinli, A., Al Mdallal, Q. (2021). A fractional-order model of COVID-19 considering the fear effect of the media and social networks on the community. *Chaos Solitons Fractals, 152,* 111403. DOI 10.1016/j.chaos.2021.111403.
37. Sindhu, T. N., Shafiq, A., Al-Mdallal, Q. M. (2021). On the analysis of number of deaths due to COVID-19 outbreak data using a new class of distributions. *Results in Physics, 21,* 103747. DOI 10.1016/j.rinp.2020.103747.

38. Shafiq, A., Lone, S. A., Sindhu, T. N., El Khatib, Y., Al-Mdallal, Q. M. et al. (2021). A new modified kies FrÃ©chet distribution: Applications of mortality rate of COVID-19. *Results in Physics, 28,* 104638. DOI 10.1016/j.rinp.2021.104638.
39. Diagne, M. L., Rwezaura, H., Tchoumi, S. Y., Tchuenche, J. M. (2021). A mathematical model of COVID-19 with vaccination and treatment. *Computational and Mathematical Methods in Medicine, 2021,* 1250129. DOI 10.1155/2021/1250129.
40. Gokbulut, N., Kaymakamzade, B., Sanlidag, T., Hincal, E. (2021). Mathematical modelling of COVID-19 with the effect of vaccine. *AIP Conference Proceedings, 2325(1),* 020065. DOI 10.1063/5.0040301.
41. Yavuz, M., CoşarÖ, F., Günay, F., Özdemir, F. N. (2021). A new mathematical modeling of the COVID-19 pandemic including the vaccination campaign. *Open Journal of Modelling and Simulation, 9(3),* 299–321. DOI 10.4236/ojmsi.2021.93020.
42. covidvax.live (2021). http://covidvax.live/ar/location/sau.
43. Gómez-Aguilar, J. F., Rosales-García, J. J., Bernal-Alvarado, J. J., Córdova-Fraga, T., Guzmán-Cabrera, R. (2012). Fractional mechanical oscillators. *Revista Mexicana de Física, 58(4),* 348–352.
44. Toufik, M., Atangana, A. (2017). New numerical approximation of fractional derivative with non-local and non-singular kernel: Application to chaotic models. *Chaos Solitons Fractals, 132,* 444. DOI 10.1140/epjp/i2017-11717-0.
45. Diethelm, K., Freed, A. D. (1998). The FracPECE subroutine for the numerical solution of differential equations of fractional order. *Forschung und Wissenschaftliches Rechnen, 1999,* 57–71.